Available online at www.sciencedirect.com
ScienceDirect
Journal of Sound and Vibration 311 (2008) 1114–1140
JOURNAL OF SOUND AND VIBRATION
www.elsevier.com/locate/jsvi

3-D free vibration analysis of annular plates on Pasternak elastic foundation via *p*-Ritz method

Sh. Hosseini Hashemi, H. Rokni Damavandi Taher, M. Omidi*

Impact Laboratory, School of Mechanical Engineering, Iran University of Science and Technology, Narmak, Tehran 16846-13114, Iran

Received 28 November 2006; received in revised form 3 October 2007; accepted 3 October 2007
Available online 26 November 2007

Abstract

In this study, a three-dimensional (3-D) free vibration analysis of thick annular plates resting on elastic foundation with different combinations of free, soft simply supported, hard simply supported and clamped boundary conditions at the inner and outer edges of the annular plate is presented on the basis of the polynomials-Ritz method. The elastic foundation is considered as a Pasternak model with adding a shear layer to the Winkler model. The analysis procedure is based on the linear, small strain, and 3-D elasticity theory. In this analysis method, a set of orthogonal polynomial series in cylindrical polar coordinate is used to extract eigenvalue equation yielding the natural frequencies and mode shapes for the annular plates. The accuracy of these results is verified by appropriate convergence studies and checked with the available literature, finite element method (FEM) analysis and the Mindlin theory. Furthermore, the effect of the foundation stiffness parameters, thickness–radius ratio, inner–outer radius ratio and different combinations of boundary conditions on the ill-conditioning of the mass matrix as well as on the vibration behavior of the annular plates is investigated. Finally, the validity and the range of applicability of the results obtained on the basis of the Mindlin and classical plate theories for a thin and moderately thick annular plate with different values of the Winkler foundation stiffness are graphically presented through comparing them with those obtained by the present 3-D *p*-Ritz solution.

1. Introduction

A plentiful number of plates resting on elastic foundations with different shapes, sizes, thickness variations and boundary conditions have been the subject of numerous investigations and those play an important role in aerospace, marine, civil, mechanical, electronic and nuclear engineering problems. For example, these types of plates are used in various kinds of industrial applications such as the analysis of reinforced concrete pavements of roads, airport runways and foundations of buildings.

An excellent survey of the research work on the free vibration of annular plates has been done by Leissa [1]. A vast amount of literature for free vibration studies of circular and annular plates have been performed with two-dimensional (2-D) theories. The natural frequencies of Mindlin annular plates under nine different combinations of free, simply supported and clamped boundary conditions have been reported by Irie et al. [2].

*Corresponding author. Tel.: +98 918 3312585; fax: +98 217 7240488.
E-mail address: m_omidi@mail.iust.ac.ir (M. Omidi).

0022-460X/$ - see front matter © 2007 Elsevier Ltd. All rights reserved.
doi:10.1016/j.jsv.2007.10.020

Such solutions are generally valid for the lower frequency, flexural modes of moderately thick plate. In recent years, the excellent studies have been done for both completely free circular and annular plates by So and Leissa [3] and circular plates with different edge boundary conditions by Liew and Yang [4] using three-dimensional (3-D) theory of elasticity. Furthermore, many different combinations of edge boundary conditions for 3-D free vibration analysis of annular plates have already been employed and studied by Rokni et al. [5] for variable thickness and Liew and Yang [6] for uniform thickness based on polynomials-Ritz analysis and by Zhou et al. [7] using Chebyshev–Ritz method.

When the shear stiffness of the foundation is considered, the two-parameter foundations, such as Filonenko-Borodich [8], Pasternak [9], generalized [10], and Vlasov and Leontev [11] foundations, can be used. A number of papers have dealt with natural frequencies of plates of uniform/non-uniform thickness, using variety of methods in order to investigate the effect of elastic foundation. Galerkin method with three terms has been employed by Bolton [12] to analyze static response of circular plates on Winkler [13] elastic foundation. Dumir [14] presented an approximate one term "space-mode solution" of the governing von Kármán-type equations for vibration analysis of thin circular plates on Winkler, Pasternak and nonlinear Winkle elastic foundation. The vibration of a plate supported laterally by an elastic foundation has been discussed on the first page of Leissa's celebrated book [15]. Leissa deduced that the effect of a full Winkler foundation merely increases the square of the natural frequency of the plate by a constant. The same conclusion was obtained by Salari et al. [16] to study the effect of Winkler elastic foundation on completely free circular plates.

Many researchers have carried out their research on the vibration of the Mindlin plates resting on elastic foundation. The vibration of polar orthotropic circular plates on an elastic foundation has been investigated by Gupta et al. [17]. The Mindlin shear deformable plate theory was employed and the Chebyshev collocation method was applied to obtain the frequency parameters for the circular plates [17]. Ju et al. [18] developed a finite element model to study the vibration of Mindlin plates with multiple stepped variations in thickness and resting on non-homogeneous elastic foundations. Frequency parameters and vibration mode shapes for stepped rectangular and circular plates resting on non-homogenous elastic foundations were presented [18].

In recent years, the Ritz method has been applied by research workers to study the plate vibration of different shapes. Gupta et al. [19,20] studied the effect of elastic foundation on axisymmetric vibrations of polar orthotropic circular plates of variable thickness by taking approximating polynomials in Rayleigh–Ritz method. Laura et al. [21] analyzed the free vibration of a solid circular plate of linearly varying thickness attached to Winkler foundation using the Ritz method. Liew et al. [22] employed the differential quadrature method for studying the Mindlin's plate on Winkler foundation. Moreover, Zhou et al. [23] described an excellent investigation of the 3-D free vibration of thick circular plates resting on Pasternak foundation by using the Chebyshev–Ritz method.

To distinguish the present work from those available in the literature, the main objective of this paper is focused on 3-D free vibration analysis of thick annular plates resting on elastic foundation with different combinations of free, soft simply supported, hard simply supported and clamped boundary conditions at the inner and outer edges by using the *p*-Ritz method. The elastic foundation is considered as a Pasternak model (two-parameter foundation) by adding a shear layer to the Winkler model in order to describe the mechanical behavior of the foundation. The polynomials-Ritz model based on sets of trigonometric functions in the circumferential direction, and algebraic polynomials in the radial and thickness directions multiplied by boundary functions is developed as the admissible functions of displacement components u, v, and w in the radial, circumferential, and thickness directions, respectively. The boundary functions are used in the admissible functions to satisfy the geometric boundary conditions of the plate.

In order to determine the number of terms in polynomial displacement functions, the convergence study firstly is carried out. Afterwards, the influence of different parameters of the annular plate as well as the number of terms used in the radial direction on the instability of the mass matrix is studied to nullify the ill-conditioning phenomenon. The presented results are compared with existing ones in the open literature [23] to show the accuracy. This comparison is also performed with the FEM analysis and the Mindlin results presented by the authors for the first time. The influence of the foundation stiffness parameters, thickness–radius ratio, inner–outer radius ratio and different combinations of boundary conditions on the frequency parameters of the plate is also studied. Moreover, the validity and the range of applicability

of the Mindlin and the CLPT results are studied for a thin and moderately thick annular plate by comparing them with those acquired by the present 3-D p-Ritz solution. The variation of the frequency parameters against the foundation stiffness parameters is also presented for various inner–outer radius ratios. Finally, 2- and 3-D plots of the mode shapes are given for different combinations of boundary conditions.

2. Theoretical formulation

Consider a thick annular plate with outer radius a_o, inner radius a_i and thicknesses h resting on Pasternak elastic foundation, as depicted in Fig. 1. The plate geometry and dimensions are defined in an orthogonal cylindrical coordinate system (r, θ, z).

For free vibrations, the displacement components of the 3-D elastic body may be expressed as

$$\begin{aligned} u(r,\theta,z,t) &= \psi_1(r,\theta,z)\,\mathrm{e}^{\mathrm{j}\omega t},\\ v(r,\theta,z,t) &= \psi_2(r,\theta,z)\,\mathrm{e}^{\mathrm{j}\omega t},\\ w(r,\theta,z,t) &= \psi_3(r,\theta,z)\,\mathrm{e}^{\mathrm{j}\omega t}, \end{aligned} \tag{1}$$

where t is the time, ω denotes the natural frequency of vibration and $\mathrm{j} = \sqrt{-1}$.

Considering the circumferential symmetry of the annular plate about the coordinate θ, the displacement amplitude functions can be written as

$$\begin{aligned} \psi_1(r,z,\theta) &= \cos(n\theta)\bar{\psi}_1(r,z),\\ \psi_2(r,z,\theta) &= \sin(n\theta)\bar{\psi}_2(r,z),\\ \psi_3(r,z,\theta) &= \cos(n\theta)\bar{\psi}_3(r,z), \end{aligned} \tag{2}$$

where the non-negative integer n represents the circumferential wavenumber of the corresponding mode shape. It is obvious that $n = 0$ means the axisymmetric vibration. Rotating the symmetry axes by $\pi/2$, another set of free vibration modes can be obtained, corresponding to an interchange $\cos(n\theta)$ and $\sin(n\theta)$ in Eq. (2). However, in such a case, $n = 0$ means representing torsional vibration.

The strain energy V of a 3-D elastic annular plate undergoing free vibration in circumferential coordinates is expressed by terms of the strains (ε_{ij}) as

$$V = (1/2)\int_{a_i}^{a_0}\int_{0}^{2\pi}\int_{-h/2}^{h/2}[\lambda(\mathbf{\Lambda}_1) + G\{2(\mathbf{\Lambda}_2) + (\mathbf{\Lambda}_3)\}]r\,\mathrm{d}r\,\mathrm{d}\theta\,\mathrm{d}z, \tag{3}$$

where λ and G are the Lame constants for a homogeneous and isotropic material, which are expressed in terms of Young's modulus E and the Poisson's ratio v by

$$\lambda = vE/[(1+v)(1-2v)], \quad G = E/[2(1+v)],$$

and

$$\mathbf{\Lambda}_1 = \varepsilon_{rr} + \varepsilon_{\theta\theta} + \varepsilon_{zz}, \quad \mathbf{\Lambda}_2 = \varepsilon_{rr}^2 + \varepsilon_{\theta\theta}^2 + \varepsilon_{zz}^2, \quad \mathbf{\Lambda}_3 = \varepsilon_{r\theta}^2 + \varepsilon_{\theta z}^2 + \varepsilon_{rz}^2. \tag{4}$$

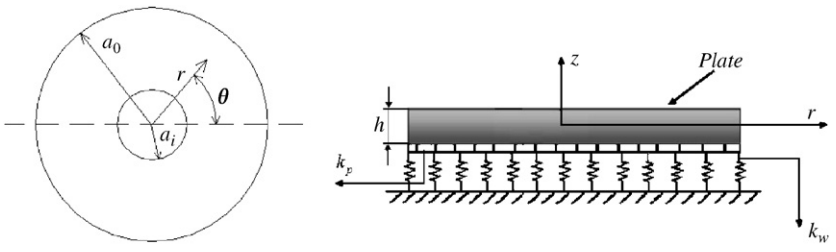

Fig. 1. Geometry and dimensions of an annular plate resting on Pasternak elastic foundation.

Using the displacement field given in Eq. (1), the strain components ε_{ij} $(i,j = r,\theta,z)$ for small deformation are defined as follows:

$$\varepsilon_{rr} = \frac{\partial u}{\partial r}, \quad \varepsilon_{\theta\theta} = \frac{1}{r}\left(u + \frac{\partial v}{\partial \theta}\right), \quad \varepsilon_{zz} = \frac{\partial w}{\partial z},$$
$$\varepsilon_{r\theta} = \frac{1}{r}\left(\frac{\partial u}{\partial \theta} + \frac{r\partial v}{\partial r} - v\right), \quad \varepsilon_{rz} = \frac{\partial u}{\partial z} + \frac{\partial w}{\partial r}, \quad \varepsilon_{\theta z} = \frac{1}{r}\left(\frac{r\partial v}{\partial z} + \frac{\partial w}{\partial \theta}\right). \tag{5}$$

The kinetic energy for free vibration is

$$\mathbf{T} = (\rho/2)\int_{a_i}^{a_o}\int_{0}^{2\pi}\int_{-h/2}^{h/2}(\dot{u}^2 + \dot{v}^2 + \dot{w}^2) r\,\mathrm{d}r\,\mathrm{d}\theta\,\mathrm{d}z, \tag{6}$$

and the strain energy owing to the Pasternak foundation model is

$$\mathbf{P} = (1/2)\int_{a_i}^{a_o}\int_{0}^{2\pi}\left(k_w(w)^2 + k_p\left(\left(\frac{\partial w}{\partial r}\right)^2 + \left(\frac{\partial w}{r\partial \theta}\right)^2\right)\right)\Bigg|_{z=-h/2} r\,\mathrm{d}r\,\mathrm{d}\theta, \tag{7}$$

where ρ is the mass density per unit volume, k_w is the Winkler foundation stiffness and k_p is constant showing the effect of shear interaction of the vertical elements.

For generality and convenience in the mathematical formulation, the following dimensionless parameters are introduced:

$$r^* = \frac{r}{a_o}, \quad z^* = \frac{z}{h}, \quad \delta = \frac{h}{a_o}, \quad R = \frac{a_i}{a_o}. \tag{8}$$

The Lagrangian energy function $\mathbf{\Pi}$ of the plate is defined as follows:

$$\mathbf{\Pi} = \mathbf{V}_{\max} - \mathbf{T}_{\max} + \bar{\mathbf{P}}, \tag{9}$$

where

$$\mathbf{V}_{\max} = \frac{Gh_o}{2a_o}\int_R^1\int_{-1/2}^{1/2}\left[\left\{\frac{\lambda}{G}\bar{\mathbf{\Lambda}}_1 + 2\bar{\mathbf{\Lambda}}_2\right\}L_1 + \bar{\mathbf{\Lambda}}_3 L_2\right] r^*\,\mathrm{d}r^*\,\mathrm{d}z^*, \tag{10}$$

$$\mathbf{T}_{\max} = \frac{1}{2}\rho\omega^2 a_o h\int_R^1\int_{-1/2}^{1/2}\left\{L_1(\bar{\psi}_1^2 + \bar{\psi}_3^2) + L_2\bar{\psi}_2^2\right\} r^*\,\mathrm{d}r^*\,\mathrm{d}z, \tag{11}$$

$$\bar{\mathbf{P}} = \left(\frac{hG}{2a_o}\right)\int_R^1\left(L_1\bar{K}_w(\bar{\psi}_3^2) + L_1\bar{K}_p\left(\left(\frac{\partial\bar{\psi}_3}{\partial r^*}\right)^2 + \left(\frac{\partial\bar{\psi}_3}{r^*\partial\theta}\right)^2\right)\right)\Bigg|_{z^*=-1/2} r^*\,\mathrm{d}r^*, \tag{12}$$

in which

$$\bar{\mathbf{\Lambda}}_1 = \bar{\varepsilon}_{r^*r^*} + \bar{\varepsilon}_{\theta\theta} + \bar{\varepsilon}_{z^*z^*},$$
$$\bar{\mathbf{\Lambda}}_2 = \bar{\varepsilon}_{r^*r^*}^2 + \bar{\varepsilon}_{\theta\theta}^2 + \bar{\varepsilon}_{z^*z^*}^2,$$
$$\bar{\mathbf{\Lambda}}_3 = \bar{\varepsilon}_{r^*\theta}^2 + \bar{\varepsilon}_{\theta z^*}^2 + \bar{\varepsilon}_{r^*z^*}^2, \tag{13}$$

$$\bar{\varepsilon}_{r^*r^*} = \frac{\partial\bar{\psi}_1}{\partial r^*}, \quad \bar{\varepsilon}_{\theta\theta}\frac{1}{r^*}\left(\bar{\psi}_1 + \frac{\partial\bar{\psi}_2}{\partial\theta}\right), \quad \bar{\varepsilon}_{z^*z^*} = \frac{\partial\bar{\psi}_3}{\delta\,\partial z^*},$$
$$\bar{\varepsilon}_{r^*\theta} = \frac{1}{r^*}\left(\frac{\partial\bar{\psi}_1}{\partial\theta} + \frac{r^*\partial\bar{\psi}_2}{\partial r^*} - \bar{\psi}_2\right), \quad \bar{\varepsilon}_{r^*z^*} = \frac{\partial\bar{\psi}_1}{\delta\,\partial z^*} + \frac{\partial\bar{\psi}_3}{\partial r^*}, \quad \bar{\varepsilon}_{\theta z^*} = \frac{1}{r^*}\left(\frac{r^*\partial\bar{\psi}_2}{\delta\,\partial z^*} + \frac{\partial\bar{\psi}_3}{\partial\theta}\right), \tag{14}$$

$$\bar{K}_w = \frac{k_w a_0^2}{hG\delta^4} = \frac{k_w a_0}{\delta^5 G}, \quad \bar{K}_p = \frac{k_p}{\delta^4 hG}. \tag{15}$$

In addition, L_1 and L_2 in Eqs. (10)–(12) are defined by

$$L_1 = \int_0^{2\pi} \cos^2(n\theta)\,\mathrm{d}\theta = \begin{cases} 2\pi & \text{if } n = 0, \\ \pi & \text{if } n \geqslant 1, \end{cases} \tag{16}$$

$$L_2 = \int_0^{2\pi} \sin^2(n\theta)\,\mathrm{d}\theta = \begin{cases} 0 & \text{if } n = 0, \\ \pi & \text{if } n \geqslant 1. \end{cases}$$

The displacement amplitude functions may be assumed in the form of double series of algebraic polynomials multiplied by boundary functions:

$$\begin{aligned} \bar{\psi}_1(r^*, z^*) &= G_1(r^*) \sum_{i=0}^{N_1} \sum_{j=0}^{N_2} a_{ij} (r^*)^i (z^*)^j, \\ \bar{\psi}_2(r^*, z^*) &= G_2(r^*) \sum_{i=0}^{N_1} \sum_{j=0}^{N_2} b_{ij} (r^*)^i (z^*)^j, \\ \bar{\psi}_3(r^*, z^*) &= G_3(r^*) \sum_{i=0}^{N_1} \sum_{j=0}^{N_2} c_{ij} (r^*)^i (z^*)^j, \end{aligned} \tag{17}$$

where

$$G_e(r^*) = H_e(r^*) I_e(r^*) \quad (e = 1, 2, 3), \tag{18}$$

in which a_{ij}, b_{ij} and c_{ij} are the undetermined coefficients; i and j are integer; N_1 and N_2 are the highest degrees taken in the double summation, and the $G_e(r^*)$; $(e = 1, 2, 3)$ are functions depending upon the geometric boundary conditions to be enforced. It should be emphasized that in the Ritz method, the displacement functions u, v and w should satisfy the geometric boundary conditions of the plate. The boundary function components in outer edge $I_e(r^*)$ and inner edge $H_e(r^*)$; $(e = 1, 2, 3)$ of annular plate corresponding to different combinations of boundary conditions used in this paper are given in Table 1.

It should be noted that Eq. (3) is only appropriate for simply supported and clamped plates in which vertical displacements are equal to zero at the edge of the plate ($r = R$ and $z = -h/2$). If there are vertical displacements, a complimentary potential energy $V^*_{\max}$, provided by the boundary spring $k_3 G$ [23], should be added into the potential energy of the plate-foundation system:

$$\mathbf{V}^*_{\max} = L_1 k_3 \psi_3^2|_{r=R, r=1, z^*=-1/2}. \tag{19}$$

The Lagrangian energy function $\mathbf{\Pi}$ of the plate is defined as follows:

$$\mathbf{\Pi} = \mathbf{V}_{\max} + \mathbf{V}^*_{\max} - \mathbf{T}_{\max} + \bar{\mathbf{P}}, \tag{20}$$

for a plate having vertical displacement at the plate edge at $r = R$, $r = 1$ and $z^* = -1/2$, while for a plate having zero vertical displacement, $\mathbf{\Pi}$ is obtained from Eq. (9).

Table 1
Boundary functions for different combinations of boundary conditions

Boundary conditions (outer–inner edges)	$I_1(r^*)$	$I_2(r^*)$	$I_3(r^*)$	$H_1(r^*)$	$H_2(r^*)$	$H_3(r^*)$
Completely free–free	1	1	1	1	1	1
Free–soft simply supported	1	1	1	1	1	$(r^* - R)$
Free–hard simply supported	1	1	1	1	$(r^* - R)$	$(r^* - R)$
Free–clamped	1	1	1	$(r^* - R)$	$(r^* - R)$	$(r^* - R)$
Soft-simply supported–soft simply supported	1	1	$(r^* - 1)$	1	1	$(r^* - R)$
Soft simply support–clamped	1	1	$(r^* - 1)$	$(r^* - R)$	$(r^* - R)$	$(r^* - R)$
Hard simply supported–free	1	$(r^* - 1)$	$(r^* - 1)$	1	1	1
Clamped–free	$(r^* - 1)$	$(r^* - 1)$	$(r^* - 1)$	1	1	1
Clamped–clamped	$(r^* - 1)$	$(r^* - 1)$	$(r^* - 1)$	$(r^* - R)$	$(r^* - R)$	$(r^* - R)$

The eigenvalue problem is formulated by minimizing the Lagrangian energy functional with respect to the arbitrary coefficients a_{ij}, b_{ij} and c_{ij}. Thus we have

$$\frac{\partial \mathbf{\Pi}}{\partial a_{ij}} = 0, \quad \frac{\partial \mathbf{\Pi}}{\partial b_{ij}} = 0, \quad \frac{\partial \mathbf{\Pi}}{\partial c_{ij}} = 0, \tag{21}$$

which in turn lead to the following eigenfrequency equation in the matrix form as

$$(\mathbf{K} - \beta^2 \mathbf{M})\mathbf{C} = \mathbf{0}, \tag{22}$$

where

$$\mathbf{K} = \begin{bmatrix} \mathbf{k}_{11} & \mathbf{k}_{12} & \mathbf{k}_{13} \\ & \mathbf{k}_{22} & \mathbf{k}_{23} \\ \text{sym} & & \mathbf{k}_{33} \end{bmatrix}, \tag{23}$$

$$\mathbf{M} = \begin{bmatrix} \mathbf{m_{11}} & 0 & 0 \\ & \mathbf{m_{22}} & 0 \\ \text{sym} & & \mathbf{m_{33}} \end{bmatrix}, \tag{24}$$

$$\mathbf{C} = \begin{Bmatrix} \mathbf{a} \\ \mathbf{b} \\ \mathbf{c} \end{Bmatrix}, \tag{25}$$

and $\beta = \omega a_o \sqrt{\rho G^{-1}} \Big/ \delta$ is the frequency parameter.

For axisymmetric mode

$$\left(\begin{bmatrix} \mathbf{k_{11}} & \mathbf{k_{13}} \\ \text{Sym} & \mathbf{k_{33}} \end{bmatrix} - \beta^2 \begin{bmatrix} \mathbf{m_{11}} & 0 \\ \text{Sym} & \mathbf{m_{33}} \end{bmatrix} \right) \begin{Bmatrix} \mathbf{a} \\ \mathbf{c} \end{Bmatrix} = \begin{Bmatrix} \mathbf{0} \\ \mathbf{0} \end{Bmatrix}, \quad n = 0, \tag{26}$$

and for torsional mode

$$([\mathbf{k_{22}}] - \beta^2 [\mathbf{m_{22}}])\{\mathbf{b}\} = \{\mathbf{0}\}, \quad n = 0, \tag{27}$$

in which $\mathbf{k}_{ij}$ and $\mathbf{m}_{ii}$ $(i,j = 1,2,3)$ are the stiffness sub-matrices and the diagonal mass sub-matrices, respectively. The column vectors **a**, **b** and **c** are determined with unknown coefficients as follows:

$$\begin{aligned} \{\mathbf{a}\} &= \left\{ a_{11} \ldots a_{1j} \quad a_{21} \ldots a_{2j} \quad \ldots \quad a_{i1} \ldots a_{ij} \right\}^{\mathrm{T}}, \\ \{\mathbf{b}\} &= \left\{ b_{11} \ldots b_{1j} \quad b_{21} \ldots b_{2j} \quad \ldots \quad b_{i1} \ldots b_{ij} \right\}^{\mathrm{T}}, \\ \{\mathbf{c}\} &= \left\{ c_{11} \ldots c_{1j} \quad c_{21} \ldots c_{2j} \quad \ldots \quad c_{i1} \ldots c_{ij} \right\}^{\mathrm{T}}, \end{aligned} \tag{28}$$

Solving eigenvalue equations (21)–(24) for $n \geqslant 1$ or Eqs. (26) and (27) for $n = 0$ yield the frequency parameters β.

3. Numerical results and discussion

Numerical solutions for 3-D vibration analysis of thick annular plates for various inner–outer radius ratio and thickness–radius ratio with different combinations of free, soft simply supported, hard simply supported and clamped outer and inner boundaries, resting on elastic foundation, are computed. For all results presented here, the Poisson ratio is assumed to be $v = 0.3$ and also, the vibration frequency ω is expressed in terms of a non-dimensional frequency parameter $\beta = \omega a_o \sqrt{\rho G^{-1}} \Big/ \delta$. In order to check the stability of the proposed approach as well as to validate the accuracy of that, some convergence tests and comparison studies are performed.

For the convergence study, the frequency parameters of the completely free annular plate resting on Pasternak elastic foundation with thickness–radius ratio $\delta = 0.2$, inner–outer radius ratio $R = 0.15$, and stiffness parameters $\bar{K}_w\bar{K}_P = (5, 1)$, (50, 5), and (100, 10) are performed in Table 2 for four circumferential wavenumbers $n = 0$, 1, 2, and 3, while the first three modes $s = 1$, 2, and 3 are considered for each value of n. Six groups of series terms are taken into account, as shown in Table 2, where N_1 means the term number used in the radial direction and N_2 means that used in the thickness direction for each displacement component. From the frequency parameters presented in this table, it can be observed that the used terms are set to be $N_1 = 10$ and $N_2 = 5$ for five significant figures.

Table 2
Convergence of the frequency parameters for a thick annular plate resting on Pasternak elastic foundation with both outer and inner edges free (F–F) for thickness–radius ratio $\delta = 0.2$ and inner–outer radius ratio $R = 0.15$

$\bar{K}_w$	$\bar{K}_P$	CWN (n)	MS (s)	$N_1 \times N_2$					
				7×5	8×5	9×5	10×5	10×6	11×5
5	1	0	1	11.029	11.029	11.029	11.029	11.029	11.029
			2	16.035	16.034	16.034	16.034	16.034	16.034
			3	21.978	21.976	21.974	21.973	21.973	21.973
		1	1	12.518	12.518	12.518	12.518	12.518	12.518
			2	13.894	13.894	13.894	13.894	13.894	13.894
			3	16.744	16.744	16.744	16.744	16.744	16.744
		2	1	10.284	10.279	10.277	10.277	10.277	10.277
			2	15.732	15.731	15.731	15.731	15.731	15.731
			3	20.521	20.519	20.518	20.518	20.518	20.518
		3	1	17.830	17.828	17.827	17.827	17.827	17.827
			2	19.780	19.780	19.780	19.780	19.780	19.780
			3	28.998	28.997	28.996	28.995	28.995	28.995
50	5	0	1	15.918	15.918	15.918	15.918	15.918	15.918
			2	31.910	31.910	31.910	31.910	31.910	31.910
			3	39.684	39.683	39.683	39.683	39.683	39.683
		1	1	13.826	13.826	13.826	13.826	13.826	13.826
			2	29.975	29.975	29.975	29.975	29.975	29.975
			3	32.777	32.777	32.777	32.777	32.777	32.777
		2	1	10.289	10.284	10.282	10.282	10.282	10.282
			2	20.423	20.421	20.420	20.420	20.420	20.420
			3	32.541	32.534	32.531	32.529	32.529	32.529
		3	1	17.844	17.841	17.840	17.840	17.840	17.840
			2	28.742	28.741	28.740	28.739	28.739	28.739
			3	39.102	39.095	39.092	39.090	39.090	39.090
100	10	0	1	15.927	15.927	15.927	15.927	15.927	15.927
			2	38.159	38.159	38.159	38.159	38.159	38.159
			3	43.669	43.669	43.668	43.668	43.668	43.668
		1	1	13.827	13.827	13.827	13.827	13.827	13.827
			2	30.691	30.691	30.691	30.691	30.691	30.691
			3	34.779	34.779	34.779	34.779	34.779	34.779
		2	1	10.290	10.285	10.283	10.282	10.282	10.282
			2	20.430	20.428	20.427	20.427	20.427	20.427
			3	32.964	32.956	32.952	32.951	32.951	32.951
		3	1	17.844	17.842	17.841	17.840	17.840	17.840
			2	28.798	28.796	28.796	28.795	28.795	28.795
			3	41.476	41.451	41.439	41.434	41.434	41.434

It is interesting to note that the convergence rate, except for circumferential wavenumber $n = 0$, is improving for frequency parameter by decreasing the stiffness parameters. Table 3 demonstrates further the convergence patterns of thick annular plate resting on the Pasternak elastic foundation with different combinations of boundary conditions (free outer edge and soft simply supported, hard simply supported and clamped inner edge), thickness–radius ratio $\delta = 0.25$, inner–outer radius ratio $R = 0.2$ and stiffness

Table 3
Convergence of the frequency parameters for a thick annular plate resting on Pasternak elastic foundation with different combinations of boundary conditions when $R = 0.2$, $\delta = 0.25$, $K_w = 10$ and $K_p = 2$

CWN (n)	MS (s)	$N_1 \times N_2$				
		7×5	8×5	9×5	10×5	10×6
An annular plate with free outer edge and soft simply supported inner edge (F–S^S)						
0	1	12.104	12.103	12.101	12.101	12.101
	2	14.485	14.485	14.485	14.485	14.485
	3	26.742	26.740	26.738	26.737	26.737
1	1	11.115	11.110	11.108	11.108	11.108
	2	13.711	13.708	13.707	13.707	13.707
	3	17.163	17.160	17.159	17.159	17.159
2	1	7.5603	7.5560	7.5556	7.5555	7.5555
	2	15.825	15.823	15.821	15.820	15.820
	3	17.055	17.050	17.048	17.048	17.048
3	1	14.019	14.017	14.015	14.015	14.015
	2	19.804	19.799	19.796	19.795	19.795
	3	23.327	23.325	23.323	23.322	23.322
An annular plate with free outer edge and hard simply supported inner edge (F–S^h)						
0	1	12.104	12.103	12.101	12.101	12.101
	2	14.485	14.485	14.485	14.485	14.485
	3	26.742	26.740	26.738	26.737	26.737
1	1	5.6505	5.6496	5.6493	5.6491	5.6491
	2	12.596	12.588	12.584	12.582	12.582
	3	13.923	13.911	13.905	13.902	13.902
2	1	9.9721	9.9710	9.9705	9.9703	9.9703
	2	16.159	16.148	16.142	16.139	16.139
	3	17.778	17.767	17.762	17.760	17.760
3	1	14.474	14.468	14.465	14.465	14.465
	2	19.822	19.809	19.803	19.800	19.800
	3	23.728	23.721	23.719	23.718	23.718
An annular plate with free outer edge and clamped inner edge (F–C)						
0	1	14.079	14.068	14.061	14.059	14.059
	2	15.538	15.531	15.528	15.527	15.527
	3	27.390	27.381	27.376	27.374	27.374
1	1	6.2329	6.2318	6.2313	6.2310	6.2310
	2	13.394	13.393	13.393	13.393	13.393
	3	14.682	14.676	14.670	14.669	14.669
2	1	10.461	10.447	10.442	10.440	10.440
	2	16.222	16.216	16.213	16.212	16.212
	3	18.084	18.073	18.066	18.063	18.063
3	1	14.586	14.580	14.578	14.577	14.577
	2	19.805	19.803	19.802	19.802	19.802
	3	23.828	23.816	23.811	23.809	23.809

parameters $\bar{K}_w = 10$ and $\bar{K}_P = 2$. The effect of different boundary conditions on the rate of convergence of the frequency parameter is shown in this table. A rapid convergence has been obtained for annular plate with free outer edge and soft simply supported inner edge (F–S^S), (i.e. 10×5 terms) in order to achieve five significant figures; while for free outer edge and hard simply supported inner edge (F–S^h) and free outer edge and clamped inner edge (F–C), frequency parameters converge to four significant figures using the same terms (i.e. 10×5 terms) of the Ritz polynomials. Although slightly higher terms are needed for free–hard simply supported and free–clamped annular plate to achieve five-digit accuracy, it is impossible to increase the order of the Ritz polynomials due to the ill-conditioning problem.

Polynomial functions are well known to be ill-conditioned, e.g., the computer can hardly find the difference between x^{10} and x^{11} within $0 < x < 1$. The ill-conditioned matrix in the polynomials–Ritz method can lead to delay convergence or produce inaccurate frequency parameters. As a consequence, finding an appropriate term number especially used in the radial direction, i.e. N_1, seems to be necessary to avoid ill-conditioning problem in the mass matrix. In order to achieve this purpose, Fig. 2 is a graph of the condition number of the mass matrix against N_1 for the annular plate resting on the Pasternak elastic foundation with thickness–radius ratio $\delta = 0.25$, inner–outer radius ratio $R = 0.2$, and stiffness parameters $\bar{K}_w\bar{K}_P = (10, 2)$ with different combinations of boundary conditions when $(n, s) = (1, 1)$. The number of terms used in the thickness direction, i.e. N_2, is taken equal to 5 in Figs. 2–5. It seems to be necessary to point out that the condition number of mass matrix for vibrating plate problems is discussed by Leung et al. [24] for the first time. The condition number is defined as the ratio of the largest singular value to the smallest singular value and is a measure of the ill-conditioning of the matrix. It can be seen in Fig. 2 that for the completely free annular plate with the term number greater than 11 and for the annular plate soft- and hard-simply supported and clamped at the inner edge and free at the outer edge with the term number greater than 10, the condition number of the mass matrix is near and above the order 10^{18} which is the limit of the precision considered in this study. In other words, for the completely free annular plate with the term number greater than 11, for instance, numerical inaccuracies in obtaining frequency parameters begin to take effect. Fig. 2 tells us why no frequency parameter is presented for free–soft simply supported, free–hard simply supported and free–clamped annular plate when N_1 and N_2 are considered to be 11 and 5, respectively.

To the best of the authors' knowledge, the effect of the Winkler foundation stiffness parameter on the ill-conditioning problem is investigated as an innovative study for various values of thickness–radius and inner–outer radius ratios with different combinations of boundary conditions, as shown in Figs. 3–5. Herein,

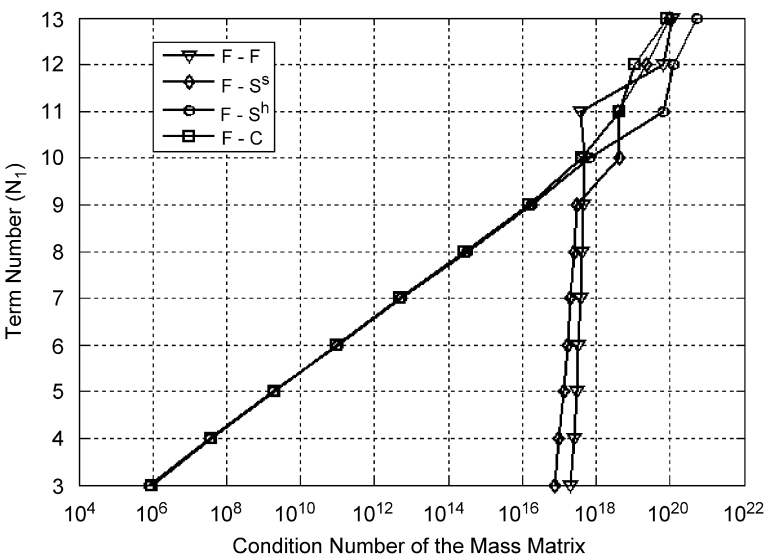

Fig. 2. The term number N_1 versus condition number of the mass matrix for completely free annular plate ($R = 0.2$) with thickness–radius ratio $\delta = 0.25$ and frequency parameters $(\bar{K}_w, \bar{K}_P) = (10, 2)$ when $(n, s) = (1, 1)$ and $N_2 = 5$. (∇) free–free plate; ($\diamond$) free–soft simply supported plate; ($\circ$) free–hard simply supported plate; ($\square$) free–clamped plate.

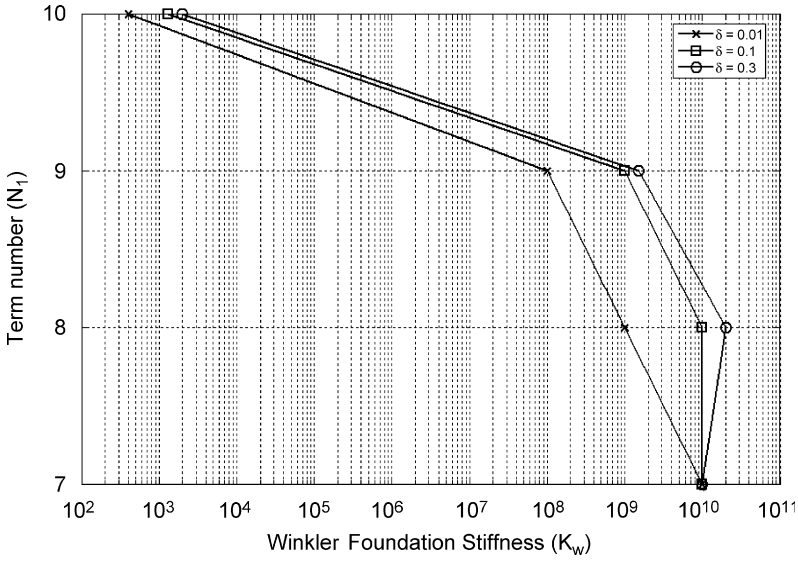

Fig. 3. The term number N_1 versus the Winkler foundation stiffness $\bar{K}_w$ for completely free annular plate ($R = 0.15$) when $(n, s) = (0, 1)$, $\bar{K}_p = 0$ and $N_2 = 5$. ($\times$) $\delta = 0.01$; ($\square$) $\delta = 0.1$; ($\circ$) $\delta = 0.3$.

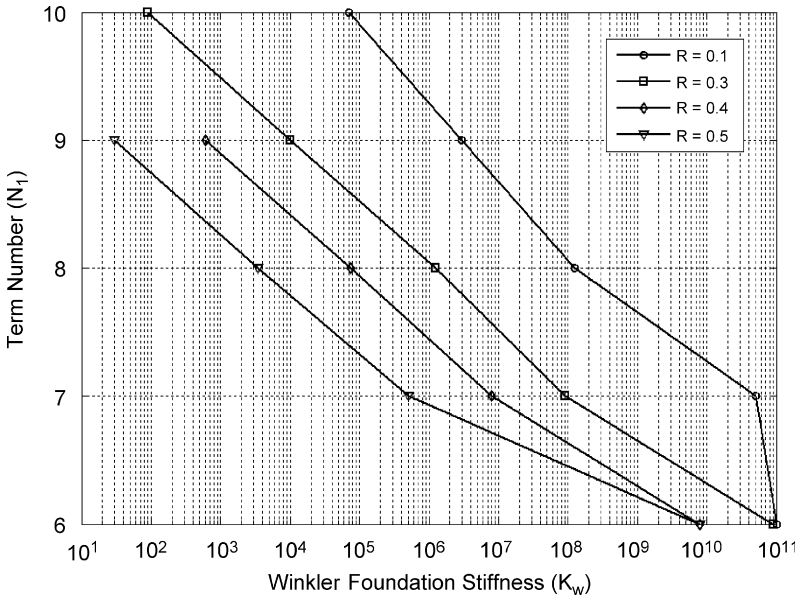

Fig. 4. The term number N_1 versus the Winkler foundation stiffness $\bar{K}_w$ for completely free annular plate with thickness–radius ratio $\delta = 0.3$ when $(n, s) = (0, 1)$, $\bar{K}_p = 0$ and $N_2 = 5$. ($\circ$) $R = 0.1$; ($\square$) $R = 0.3$; ($\diamond$) $R = 0.4$; ($\triangledown$) $R = 0.5$.

$\bar{K}_{wi}$ is defined as the largest $\bar{K}_w$ for which the mass matrix deals with no ill-conditioning problem for the selected terms of the Ritz polynomials. The primary conclusion drawn from Figs. 3–5 is that $\bar{K}_{wi}$ will decrease with the increase of the term number N_1.

Fig. 3 shows the variation of the Winkler foundation stiffness with the term number N_1 for different values of thickness–radius ratio. It is worthwhile to mention that the enhancement of the thickness–radius ratio results in increasing the values of $\bar{K}_{wi}$.

From Fig. 4, it is figured out that as the inner–outer radius ratio is diminished, the values of $\bar{K}_{wi}$ increase. When the number of terms used in the radial direction is considered to be 10 for the inner–outer radius ratio

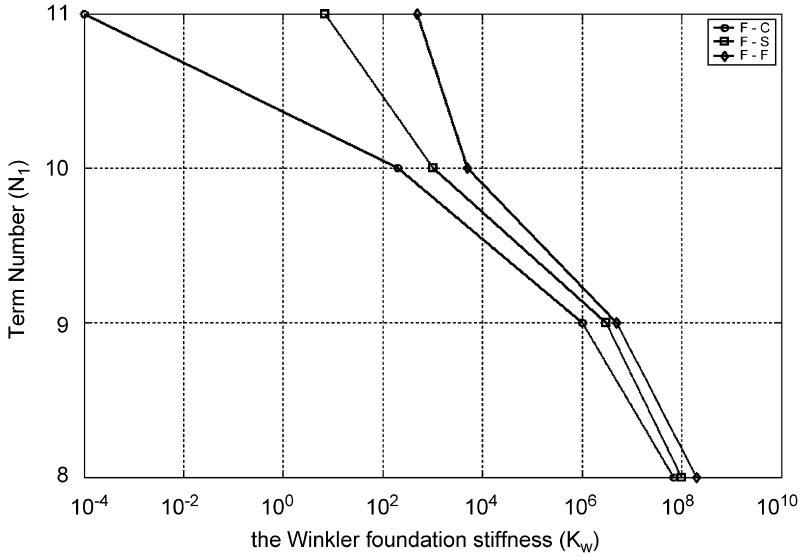

Fig. 5. The term number N_1 versus the Winkler foundation stiffness $\bar{K}_w$ for an annular plate ($R = 0.15$) with thickness–radius ratio $\delta = 0.3$ when $(n, s) = (0, 1)$, $\bar{K}_p = 0$ and $N_2 = 5$: (○) free–clamped plate; (□) free–simply supported plate; (◇) free–free plate.

Table 4
The number of terms used in this paper for different combinations of boundary conditions

Boundary conditions (outer–inner edges)	F–F	F–S^S	F–S^h	F–C
Term number used in radial direction N_1	10	10	9	9
Term number used in thickness direction N_2	5	5	5	5
Number of significant figures	5	5	4	4

0.4 and 0.5, the Winkler foundation stiffness $\bar{K}_w$ is very close to zero to nullify the ill-conditioning problem in the mass matrix.

In Fig. 5, with the increase of the edge constraint (in the order from free to simply supported to clamped), the values of $\bar{K}_{wi}$ will reduce.

It should be pointed out that a delicate balance between the high accuracy of the frequency parameter and the amount of the Winkler foundation stiffness $\bar{K}_w$ needs to be taken into account for different values of the term number N_1. For example, when the Winkler foundation stiffness is changed from 100 to 1000 for an annular plate with the free outer edge and clamped inner edge, the term number N_1 must be taken equal to 9 instead of 10 to avoid the ill-conditioning problem in the mass matrix. However, the accuracy of the frequency parameter will decrease. Considering Tables 1 and 2 as well as Figs. 2–5, the values of the term number are selected according to Table 4 for different combinations of boundary conditions so that the next results presented in this paper have an acceptable accuracy without any ill-conditioning for the mass matrix.

The 3-D free vibrations of thick circular plate ($R = 10^{-30}$) resting on Pasternak elastic foundation with different boundary conditions, thickness–radius ratio $\delta = 0.25$, and stiffness parameters $\bar{K}_w\bar{K}_P = (10, 1)$ and (100, 10) are presented in Table 5 together with the published values of Zhou et al. [23]. Note that the frequency results of Zhou et al. [23] are obtained from a Chebyshev–Ritz method. From Table 5, it is found that the present 3-D p-Ritz solution for this kind of plate is in close agreement with Chebyshev–Ritz solution.

An interesting comparison study of the 3-D and the Mindlin results with the converged finite element solutions is shown in Table 6 for an annular plate resting on the Winkler foundation with different combinations of boundary conditions, thickness–radius ratio $\delta = 0.1$, inner–outer radius ratio $R = 0.15$ and

Table 5
Comparison of the frequency parameters of circular plates with different boundary conditions between the present 3-D p-Ritz solution and the 3-D Chebyshev–Ritz method [23] when $R = 10^{-30}$ and $\delta = 0.25$

CWN (n)	MS (s)	$\bar{K}_w = 10$, $\bar{K}_p = 1$		$\bar{K}_w = 100$, $\bar{K}_p = 10$	
		[23]	Authors	[23]	Authors
Circular plate with completely free edge					
0	1	13.640	13.642	13.676	13.679
	2	25.256	25.259	32.176	32.180
	3	28.968	28.980	36.376	36.381
1	1	10.912	10.930	10.916	10.930
	2	22.548	22.553	23.112	23.116
	3	26.876	26.888	27.148	27.166
2	1	9.3800	9.3901	9.3800	9.3901
	2	16.870	16.872	16.860	16.877
	3	27.464	27.479	29.252	29.270
Circular plate with hard simply supported edge					
0	1	13.664	13.673	13.696	13.701
	2	26.412	26.421	32.228	32.235
	3	29.940	29.952	40.580	40.601
1	1	4.6480	4.6409	4.6480	4.6409
	2	21.236	21.239	21.238	21.243
	3	23.132	23.143	23.644	23.656
2	1	9.7001	9.7100	9.7001	9.7100
	2	26.680	26.701	26.682	26.699
	3	28.720	28.762	30.640	30.660
Circular plate with clamped edge					
0	1	24.328	24.339	25.320	25.340
	2	28.004	28.015	38.160	38.185
	3	33.992	34.012	42.028	42.039
1	1	13.320	13.330	13.324	13.333
	2	21.464	21.348	21.472	21.475
	3	29.200	29.301	32.760	32.772
2	1	20.652	20.663	20.672	20.680
	2	27.392	27.400	27.480	27.490
	3	32.932	32.965	37.200	37.246

stiffness parameters $\bar{K}_P = 0$ and $\bar{K}_w = 0.1$, 1 and 3. The Mindlin results have five-digit accuracy and the shear correction factor of $K^2 = \pi^2/12$ is assumed. The formulation based on the Mindlin plate theory has been presented in Appendix A.

A well-known commercially available FEM package was used for the extraction of the frequency parameters. Before proceeding to the cases for which frequency parameters are calculated for the first time, the package as well as the solution procedure were examined by solving some problems of the literature. It was seen that there is an excellent agreement between results of the FEM package and those of the literature. 3-D solid elements having all six degrees of freedom and 1-D spring elements having two degrees of freedom were adopted in all of our FEM calculations. A convergence study was conducted to ensure that results of the calculations are independent from the number of elements. The number of elements for modeling of circular plates was supposed about 14,000. Furthermore, the number of spring elements for modeling of the Winkler elastic foundation was selected about 2500.

It is observed that the present results (3-D and Mindlin solutions) are in good agreement with the finite element solutions.

Table 6
Comparison of the frequency parameters of annular plate with free–free boundary conditions among the 3-D solution, Mindlin theory and FEM when $R = 0.15$ and $\delta = 0.1$

CWN (n)	MS (s)	Method	$\bar{K}_w$		
			0.1	1	3
0	1	FEM	5.1945	10.747	17.310
		3-D	5.1867	10.727	17.285
		Mindlin	5.1894	10.746	17.320
	2	FEM	18.345	20.533	24.731
		3-D	18.337	20.501	24.625
		Mindlin	18.334	20.537	24.738
	3	FEM	32.142	32.152	32.221
		3-D	32.037	32.040	32.050
		Mindlin	–	–	–
1	1	FEM	9.9002	13.627	17.284
		3-D	9.8923	13.590	17.259
		Mindlin	9.8948	13.628	17.292
	2	FEM	25.205	26.766	27.708
		3-D	25.122	26.729	27.695
		Mindlin	25.115	26.765	–
	3	FEM	27.691	27.691	30.005
		3-D	27.691	27.692	29.983
		Mindlin	–	–	30.111
2	1	FEM	4.0341	10.267	17.420
		3-D	4.0222	10.253	17.380
		Mindlin	4.0239	10.266	17.425
	2	FEM	16.155	18.634	20.606
		3-D	16.145	18.591	20.523
		Mindlin	16.145	18.636	–
	3	FEM	20.604	20.605	23.224
		3-D	20.523	20.523	23.103
		Mindlin	–	–	23.233
3	1	FEM	6.6708	11.532	18.135
		3-D	6.6646	11.511	18.097
		Mindlin	6.6679	11.534	18.161
	2	FEM	23.718	25.439	28.903
		3-D	23.714	25.408	28.807
		Mindlin	23.707	25.448	28.946
	3	FEM	35.724	35.724	35725
		3-D	35.679	35.679	35.679
		Mindlin	–	–	–

On the basis of the present 3-D Ritz formulation, some numerical results are given in Tables 7 and 8 for annular plates resting on Pasternak elastic foundation with variable inner–outer radius and thickness–radius ratios, several values of the foundation stiffness parameters, and different combinations of boundary conditions. The frequency parameters for these annular plates with both outer and inner edges free (F–F) as well as hard simply supported outer edge and free inner edge (S^h–F) are shown in Table 7, while thickness–radius ratios $\delta = 0.15$ and 0.35, inner–outer radius ratios $R = 0.1$ and 0.3 and stiffness parameters $\bar{K}_w\bar{K}_P = (0, 0)$, (100, 10) and (1000, 100) are considered. The results of frequency parameters for other combinations of boundary conditions, including soft simply supported in both edges (S^S–S^S) and soft simply

Table 7
The frequency parameters of annular plates resting on Pasternak elastic foundations with different thickness–radius ratio, inner-outer radius ratio, stiffness parameters and combinations of boundary conditions

δ	CWN (n)	MS (s)	$(\bar{K}_w, \bar{K}_p)$					
			$R = 0.1$			$R = 0.3$		
			(0, 0)	(10^2, 10^1)	(10^3, 10^2)	(0, 0)	(10^2, 10^1)	(10^3, 10^2)
Annular plates with both outer and inner edges free (F–F)								
0.15	0	1	4.1501	22.185	22.191	3.9441	18.141	18.142
		2	16.513	54.668	55.555	18.164	53.467	54.893
		3	22.254	61.184	83.706	21.151	62.287	91.646
	1	1	9.1657	18.326	18.326	7.8819	18.856	18.857
		2	18.336	40.454	40.584	18.870	43.876	44.004
		3	23.524	45.891	45.914	23.431	51.137	52.066
	2	1	2.5044	14.727	14.727	2.3013	10.193	10.194
		2	14.713	27.687	27.691	10.188	27.136	27.140
		3	15.014	45.813	45.904	14.105	48.683	48.888
	3	1	5.7258	23.961	23.961	5.6331	21.305	21.306
		2	21.641	38.699	38.718	20.926	37.442	37.453
		3	23.963	58.713	58.983	21.297	51.974	52.129
0.35	0	1	3.7086	9.3064	9.3256	3.5024	7.7076	7.7119
		2	9.4978	17.542	18.600	7.7708	17.212	18.044
		3	12.122	18.080	19.364	15.048	17.316	19.263
	1	1	7.2459	7.8231	7.8251	6.0168	8.0402	8.0430
		2	7.8523	15.393	15.919	8.0788	16.208	17.169
		3	15.533	16.753	18.576	15.945	16.469	18.344
	2	1	2.2901	6.3228	6.3230	2.0817	4.3887	4.3895
		2	6.3139	11.720	11.742	4.3703	11.507	11.524
		3	10.993	16.759	17.708	10.215	16.651	16.843
	3	1	4.8676	10.261	10.261	4.7757	9.1543	9.1552
		2	10.268	15.609	15.859	9.1341	15.434	15.611
		3	14.686	18.622	19.561	14.266	17.802	18.591
Annular plates with hard simply supported outer edge and free inner edge (S^h–F)								
0.15	0	1	2.3292	22.206	22.210	2.2413	18.161	18.162
		2	13.032	55.379	55.575	16.082	54.615	54.924
		3	22.264	71.326	83.829	18.175	73.922	91.861
	1	1	6.4127[a]	7.7911[a]	7.7961[a]	5.7339	8.2907	8.2962
		2	7.7862	36.124	36.124	8.2853	36.995	37.013
		3	19.763	40.881	41.034	18.712	47.046	47.323
	2	1	11.320	15.107	15.111	10.343[a]	10.354[a]	10.359[a]
		2	15.088	41.122	41.129	10.768	42.204	42.210
		3	27.456	53.720	54.234	25.228	53.702	54.270
	3	1	17.079	23.984	23.987	16.626	21.406	21.409
		2	23.980	52.713	52.714	21.391	46.198	46.207
		3	35.439	66.123	67.710	33.366	65.305	66.661
0.35	0	1	2.1789	9.3315	9.3445	2.1073	7.7291	7.7316
		2	9.5072	18.810	19.347	7.7805	17.948	19.292
		3	9.9891	19.258	21.402	11.940	19.675	20.210
	1	1	3.3439[a]	3.3527[a]	3.3552[a]	3.5585[a]	3.5679[a]	3.5706[a]
		2	5.3938	15.403	15.479	4.6998	15.263	15.492)
		3	13.629	15.498	15.958	13.109	17.337	18.201

Table 7 (*continued*)

δ	CWN (n)	MS (s)	$(\bar{K}_w, \bar{K}_p)$					
			$R = 0.1$			$R = 0.3$		
			(0, 0)	$(10^2, 10^1)$	$(10^3, 10^2)$	(0, 0)	$(10^2, 10^1)$	$(10^3, 10^2)$
	2	1	6.4806[a]	6.4977[a]	6.4995[a]	4.4438[a]	4.4707[a]	4.4738[a]
		2	8.8067	17.317	17.481	8.3736	17.394	17.734
		3	17.629	18.321	18.941	16.383	18.524	18.966
	3	1	10.282[a]	10.287[a]	10.288[a]	9.1798[a]	9.2082[a]	9.2101[a]
		2	12.338	20.326	20.952	12.056	19.213	19.387
		3	22.032[a]	22.612[a]	22.619[a]	19.793	20.754	21.198

[a]0 = symmetric mode.

Table 8
The frequency parameters of annular plates resting on Pasternak elastic foundations with different thickness–radius ratio, inner–outer radius ratio, stiffness parameters and different combinations of boundary conditions

δ	CWN (n)	MS (s)	$(\bar{K}_w, \bar{K}_p)$					
			$R = 0.1$			$R = 0.3$		
			(0, 0)	$(10^2, 10^1)$	$(10^3, 10^2)$	(0, 0)	$(10^2, 10^1)$	$(10^3, 10^2)$
Annular plates with soft simply supported in both edges (S^S–S^S)								
0.15	0	1	6.4813	22.270	22.273	9.4531	18.246	18.248
		2	20.971	55.768	55.956	18.218	54.948	55.059
		3	22.294	78.177	84.681	31.354	91.122	92.139
	1	1	7.1325	18.371	18.381	10.149	18.911	18.924
		2	18.367	40.468	40.599	18.907	43.927	44.053
		3	22.265	45.904	45.925	32.066	46.286	51.588
	2	1	11.246	14.751	14.753	10.238[a]	10.262[a]	10.273[a]
		2	14.739	27.810	27.831	12.666	27.243	27.263
		3	27.671	45.966	46.057	27.233	41.091	49.013
	3	1	16.844	23.981	23.984	17.146	21.395	21.405
		2	23.976	38.923	38.957	21.363	37.633	37.658
		3	35.299	58.893	59.108	30.839	44.800	52.445
0.35	0	1	5.0064	9.4362	9.4420	7.3648[a]	7.8434[a]	7.8440[a]
		2	9.5401	19.060	20.086	7.8245	14.871	19.332
		3	14.047	21.782	22.621	19.817	21.445	25.532
	1	1	5.7444	7.8861	7.8912	7.7921	8.1246	8.1299
		2	7.8816	15.428	15.939	8.1152	16.629	17.422
		3	15.068	19.425	19.531	18.837	19.991	20.533
	2	1	6.3248[a]	6.3320[a]	6.3325[a]	4.4094[a]	4.4340[a]	4.4378[a]
		2	8.6775	11.941	11.951	9.4413	11.706	11.714
		3	11.936	17.416	17.955	11.692	17.574	18.209
	3	1	10.281[a]	10.286[a]	10.287[a]	9.1813[a]	9.2082[a]	9.2113[a]
		2	12.098	16.595	16.617	12.224	16.148	16.159
		3	16.701	20.197	20.783	13.131	19.174	19.797
Annular plates with soft simply supported outer edge and clamped inner edge (S^S–C)								
0.15	0	1	7.5948	23.526	23.530	12.335	27.194	27.200
		2	22.674	61.354	61.696	27.188	73.475	74.629
		3	23.555	78.660	91.859	34.623	87.963	104.75

Table 8 (*continued*)

δ	CWN (n)	MS (s)	$(\bar{K}_w, \bar{K}_p)$					
			$R = 0.1$			$R = 0.3$		
			(0, 0)	(10^2, 10^1)	(10^3, 10^2)	(0, 0)	(10^2, 10^1)	(10^3, 10^2)
	1	1	8.2282[a]	8.4781[a]	8.4816[a]	6.6763	12.266	12.269
		2	8.4685	21.730	21.745	12.260	26.690	26.714
		3	21.731	43.998	44.144	12.841	48.752	48.856
	2	1	11.549	16.099	16.099	14.698	19.453	19.457
		2	16.095	28.648	28.673	19.443	30.688	30.723
		3	28.466	52.714	53.012	30.709	58.485	59.115
	3	1	16.870	24.043	24.046	18.287	25.338	25.342
		2	24.039	38.980	39.015	25.330	39.722	39.765
		3	35.431	59.880	60.144	39.763	67.018	68.430
0.35	0	1	5.3595	9.9410	9.9486	8.2163	11.539	11.544
		2	10.078	19.523	20.660	11.656	20.675	21.667
		3	14.274	21.961	22.776	20.173	25.750	25.916
	1	1	3.6375[a]	3.6475[a]	3.6489[a]	5.2624[a]	5.2715[a]	5.2731[a]
		2	6.2154	9.2971	9.3055	8.6758	11.379	11.390
		3	9.3233	16.631	17.392	11.459	18.421	19.280
	2	1	6.9003[a]	6.9023[a]	6.9025[a]	8.3410[a]	8.3510[a]	8.3522[a]
		2	8.8201	12.274	12.285	10.177	13.102	13.118
		3	12.295	18.140	18.960	13.172	19.350	20.400
	3	1	10.307[a]	10.312[a]	10.313[a]	10.863[a]	10.871[a]	10.872[a]
		2	12.109	16.614	16.637	12.629	16.872	16.900
		3	16.725	20.250	20.847	17.044	20.914	21.594

[a]0 = symmetric mode.

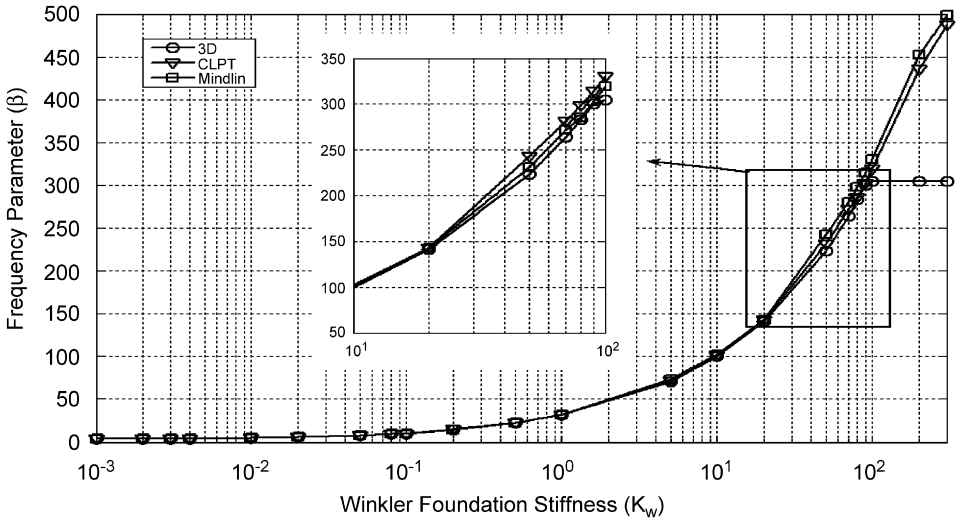

Fig. 6. The frequency parameter β versus the Winkler foundation stiffness $\bar{K}_w$ for a thin annular plate ($\delta = 0.01$ and $R = 0.2$) with both edges (outer and inner) free when (n, s) = (0, 1). (○) 3-D p-Ritz solution; (▽) classical plate theory; (□) Mindlin plate theory.

supported outer edge and clamped inner edge (S^S–C) are also given in Table 8 with the same values of ($\bar{K}_w, \bar{K}_P, \delta, R$) in Table 7. From Tables 7 and 8, it can be concluded that the frequency parameters β for all cases increase as the foundation stiffness parameters increase while those decrease as inner–outer radius ratio

increases. Furthermore, the frequency parameters decrease as higher degree of edge constraint (in the order from free to simply supported to clamped) are applied to the above-mentioned annular plates.

In Figs. 6–11, in order to determine the validity and the range of applicability of the Mindlin and classical plate results with respect to the change of the Winkler foundation stiffness $\bar{K}_w$, the results of the present 3-D analysis, the Mindlin theory and the classical plate solution are compared for thin annular plate ($\delta = 0.01$ and $R = 0.2$) with free–free and free–soft simply supported boundary condition at outer–inner edges when stiffness parameters $\bar{K}_w \neq 0$ and $\bar{K}_P = 0$. It can apparently be observed that unlike the 3-D results, the frequency parameters in the Mindlin and the classical plate theories diverge with increasing $\bar{K}_w$. It is worthwhile to mention that the classical plate theory has lower sensitivity to the Winkler foundation stiffness $\bar{K}_w$ than the Mindlin theory. In other words, as the Winkler foundation stiffness increases, the CLPT curve can follow the 3-D one better in comparison with the Mindlin results for a thin annular plate.

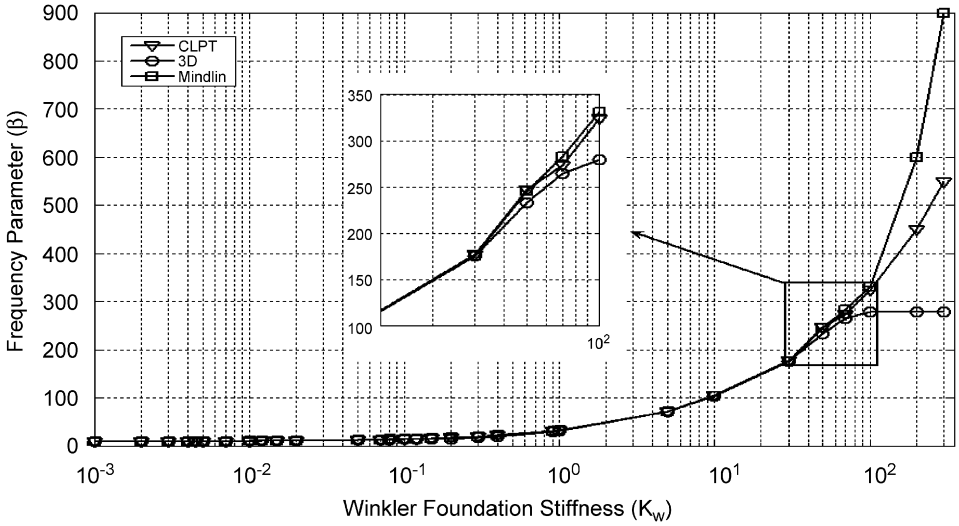

Fig. 7. The frequency parameter β versus the Winkler foundation stiffness $\bar{K}_w$ for a thin annular plate ($\delta = 0.01$ and $R = 0.2$) with both edges (outer and inner) free when $(n, s) = (1, 1)$: (○) 3-D p-Ritz solution; (▽) classical plate theory; (□) Mindlin plate theory.

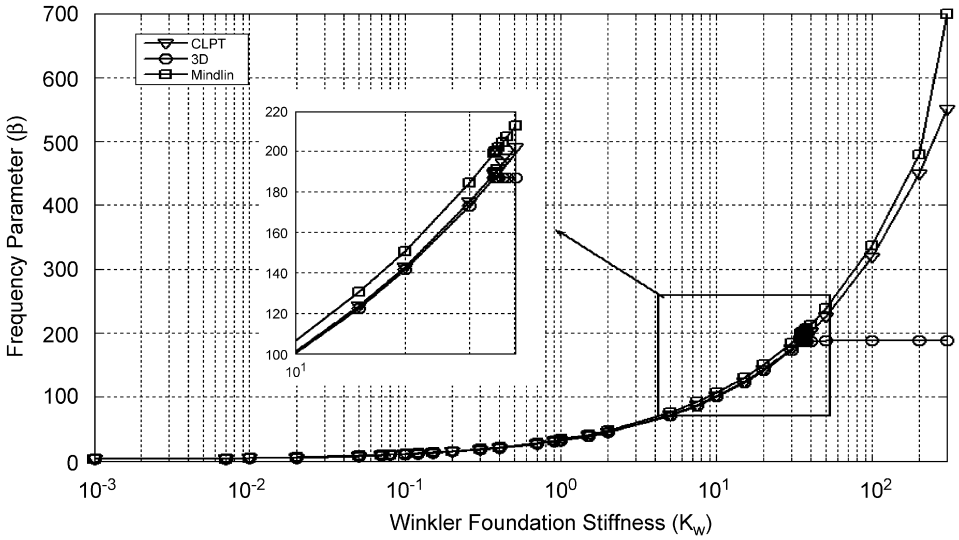

Fig. 8. The frequency parameter β versus the Winkler foundation stiffness $\bar{K}_w$ for a thin annular plate ($\delta = 0.01$ and $R = 0.2$) with both edges (outer and inner) free when $(n, s) = (2, 1)$. (○) 3-D p-Ritz solution; (▽) classical plate theory; (□) Mindlin plate theory.

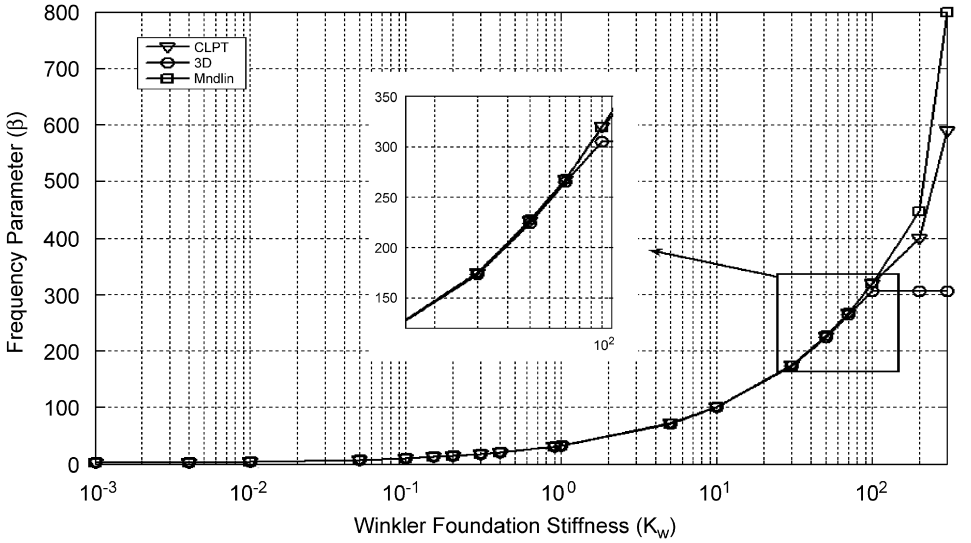

Fig. 9. The frequency parameter β versus the Winkler foundation stiffness $\bar{K}_w$ for a thin annular plate ($\delta = 0.01$ and $R = 0.2$) with free–soft simply supported at outer–inner edges when $(n, s) = (0, 1)$. (○) 3-D p-Ritz solution; (▽) classical plate theory; (□) Mindlin plate theory.

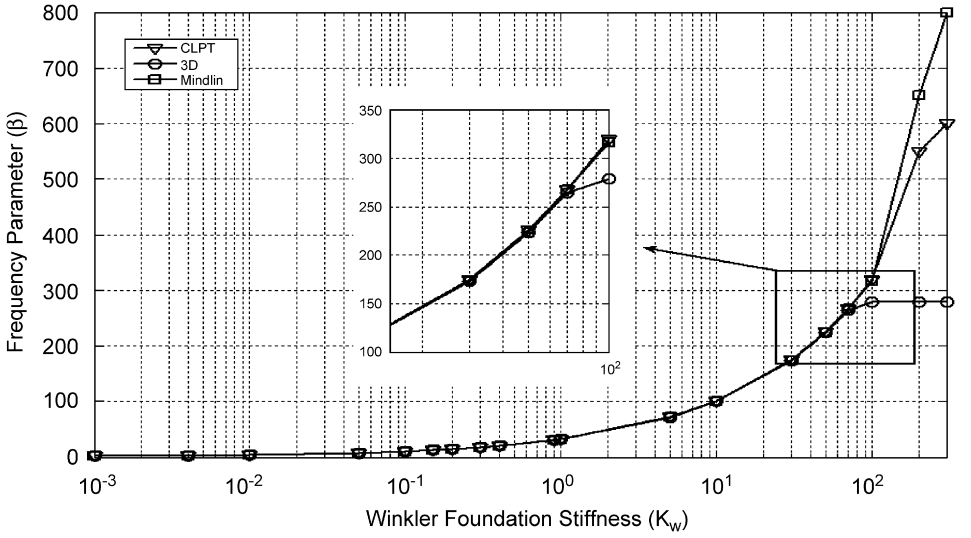

Fig. 10. The frequency parameter β versus the Winkler foundation stiffness $\bar{K}_w$ for a thin annular plate ($\delta = 0.01$ and $R = 0.2$) with free–soft simply supported at outer–inner edges when $(n, s) = (1, 1)$. (○) 3-D p-Ritz solution; (▽) classical plate theory; (□) Mindlin plate theory.

In Figs. 12–14, the similar analyses to the ones presented in Figs. 6–11 is performed for a moderately thick annular plate ($\delta = 0.15$ and $R = 0.2$) with free boundary condition at both edges and stiffness parameters $\bar{K}_w \neq 0$ and $\bar{K}_P = 0$. In these figures, the curves of the frequency parameter β versus $\bar{K}_w$ are shown to compare the results of the 3-D and the Mindlin solutions. Herein, the critical Winkler foundation stiffness $\bar{K}_{wc}$ is defined as the largest $\bar{K}_w$ in which the frequency parameters obtained from the Mindlin theory have a 10% difference from the ones acquired by the present 3-D analysis method. From Figs. 12–14, it can be seen that the frequency parameters in the Mindlin results diverge from ones in the 3-D results when $\bar{K}_w > \bar{K}_{wc}$, while the frequency parameters in 3-D solution converge to the constant values. It should be pointed out that

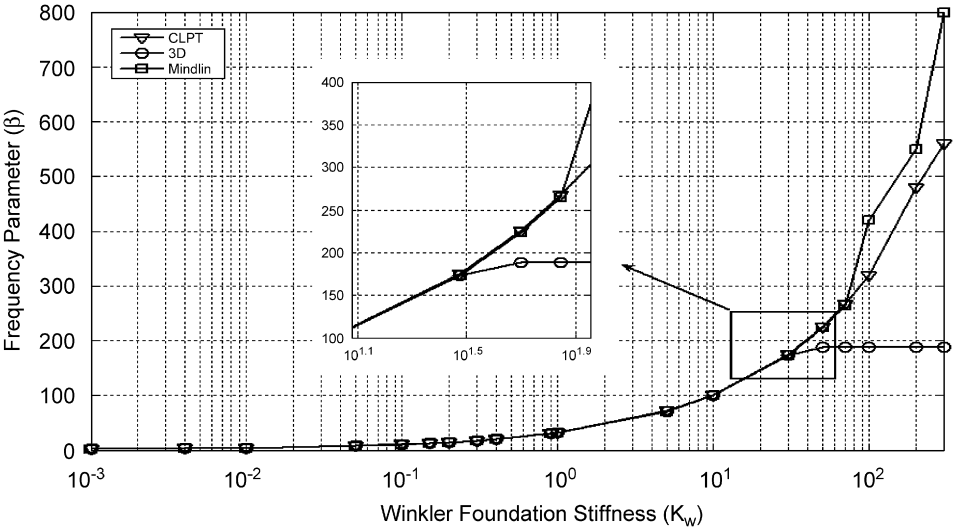

Fig. 11. The frequency parameter β versus the Winkler foundation stiffness $\bar{K}_w$ for a thin annular plate ($\delta = 0.01$ and $R = 0.2$) with free–soft simply supported at outer–inner edges when $(n, s) = (2, 1)$. (○) 3-D p-Ritz solution; (▽) classical plate theory; (□) Mindlin plate theory.

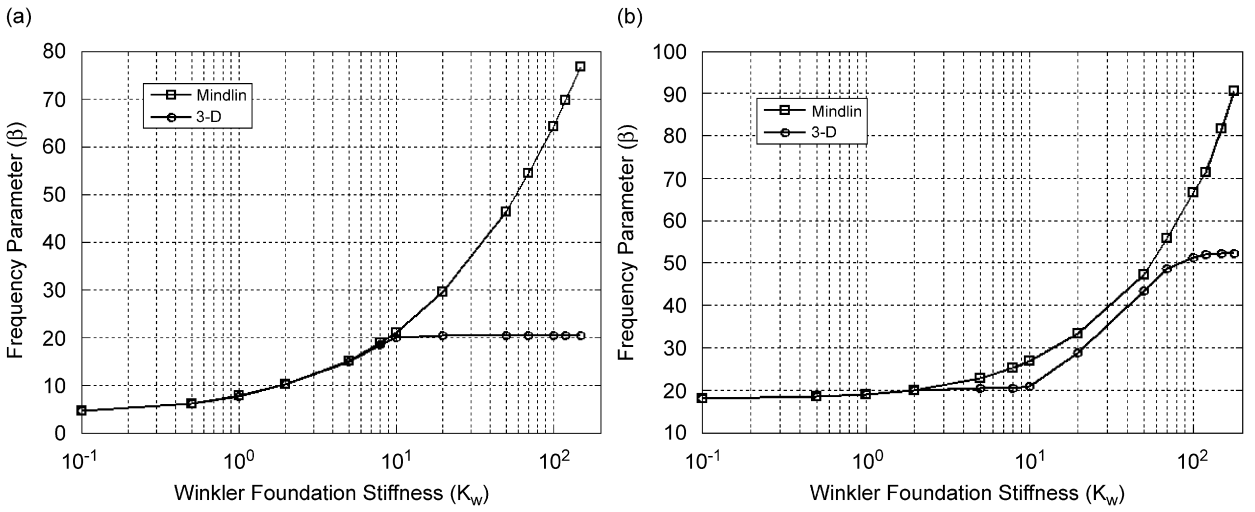

Fig. 12. The frequency parameter β versus Winkler foundation stiffness $\bar{K}_w$ for moderately thick annular plate ($R = 0.2$) with both edges (outer and inner) free and thickness–radius ratio $\delta = 0.15$. (a) $(n, s) = (0, 1)$; (b) $(n, s) = (0, 2)$. (□) Mindlin plate theory; (○) 3-D p-Ritz solution.

in the Mindlin theory, the foundation is applied on the middle surface of the plate but not on the lower surface. That is why the Mindlin theory gives incorrect results as the Winkler foundation stiffness takes the large values. In Figs. 12–14, for moderately thick annular plate with both edges free, the values of the critical Winkler foundation stiffness $\bar{K}_{wc}$ are about 9.38 and 1.17 when $(n, s) = (0, 1)$ and (0, 2), 7.52 and 5.49 when $(n, s) = (1, 1)$ and (1, 2) as well as 1.54 and 11.32 when $(n, s) = (2, 1)$ and (2, 2).

The variation of the frequency parameters against the Winkler foundation stiffness $\bar{K}_w$ is presented in Figs. 15–17 for an annular plate resting on Winkler elastic foundation ($\bar{K}_w \neq 0$, $\bar{K}_P = 0$) with both edges free while the inner–outer radius ratio is selected from 0.1 to 0.4 and thickness–radius ratio δ is set to be 0.1. Each curve in these figures has 18 sample points.

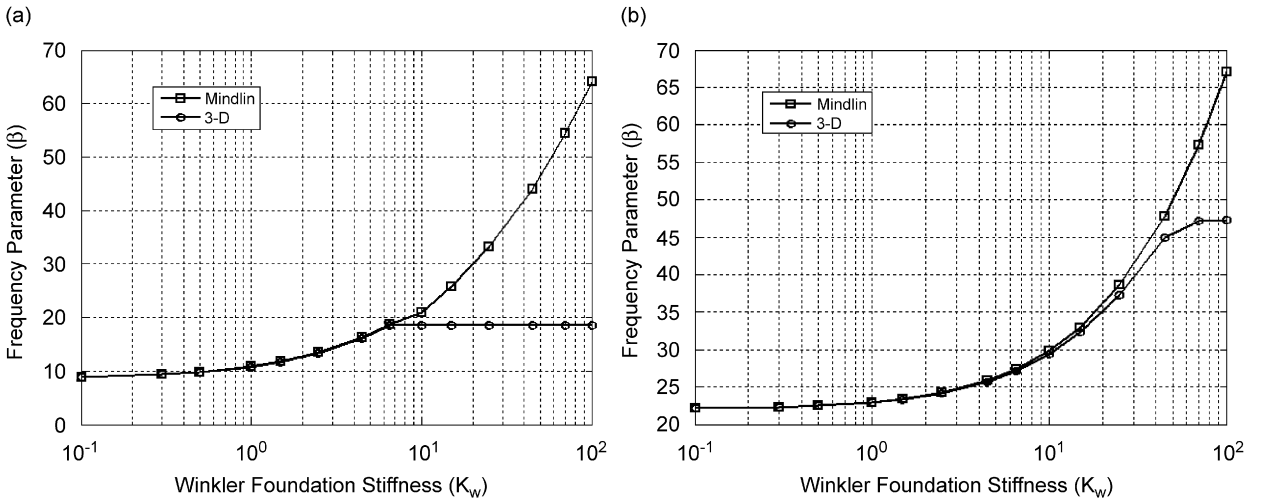

Fig. 13. The frequency parameter β versus Winkler foundation stiffness $\bar{K}_w$ for moderately thick annular plate ($R = 0.2$) with both edges (outer and inner) free and thickness–radius ratio $\delta = 0.15$. (a) $(n, s) = (1, 1)$; (b) $(n, s) = (1, 2)$. (□) Mindlin plate theory; (○) 3-D p-Ritz solution.

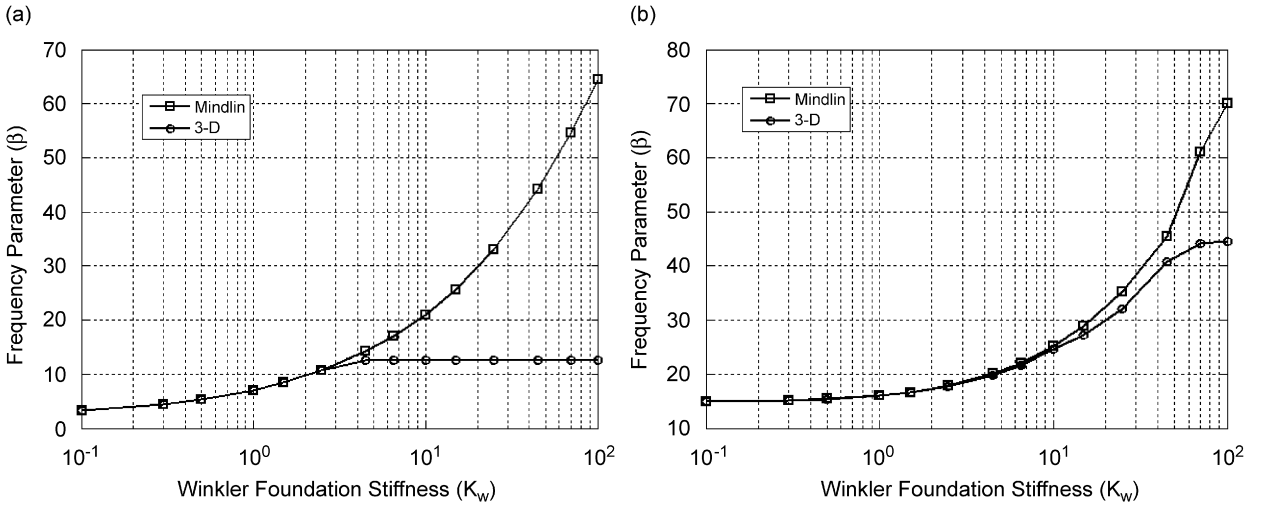

Fig. 14. The frequency parameter β versus Winkler foundation stiffness $\bar{K}_w$ for moderately thick annular plate ($R = 0.2$) with both edges (outer and inner) free and thickness–radius ratio $\delta = 0.15$. (a) $(n, s) = (2, 1)$; (b) $(n, s) = (2, 2)$. (□) Mindlin plate theory; (○) 3-D p-Ritz solution.

Fig. 15 shows the relationship between the frequency parameter β and the Winkler foundation stiffness $\bar{K}_w$ for various values of the inner–outer radius ratio. As it is expected, the frequency parameter increases with increasing $\bar{K}_w$. It will also be predictable that the frequency parameter for a given Winkler foundation stiffness becomes smaller when the inner–outer radius ratio increases, as shown in Fig. 15(a). However, considering Fig. 15(b), it is worth noting that for vibrating mode $(n, s) = (0, 2)$, the frequency parameter in the some ranges of the Winkler foundation stiffness becomes larger as the inner–outer radius ratio increases. Moreover, this phenomenon can be seen in the vibrating modes $(n, s) = (1, 1)$ and $(1, 2)$ in Fig. 16. The most effective range of the Winkler foundation stiffness in increasing the frequency parameters is from 1 to 10^1 for Fig. 15(a) and from 10^1 to 10^2 for Fig. 15(b). The effective ranges of the $\bar{K}_w$ in the increase of the frequency parameters can also be seen for the other vibrating modes in Figs. 16 and 17.

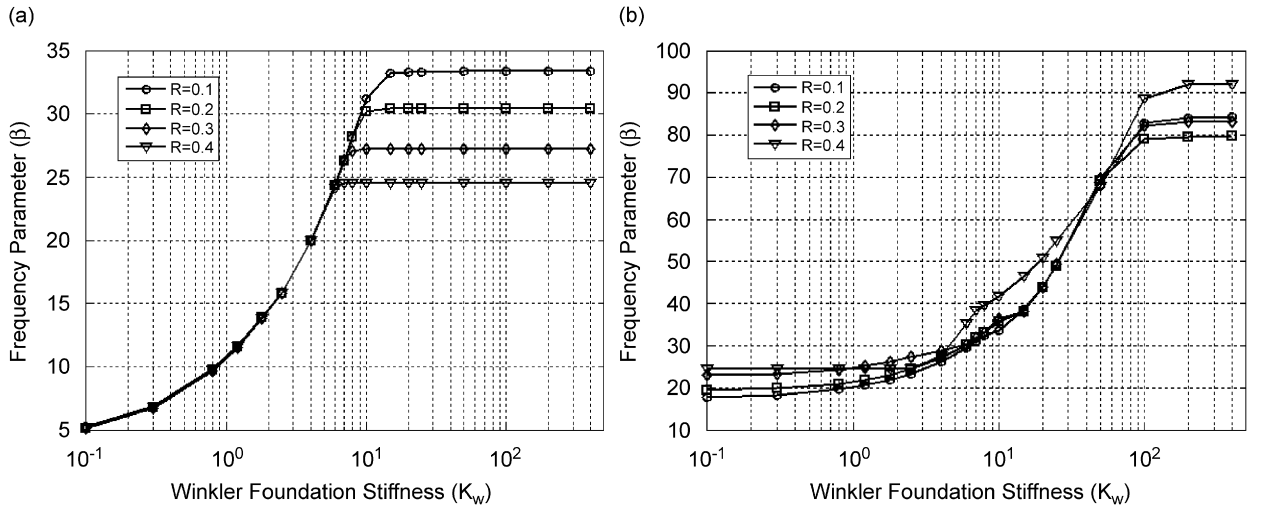

Fig. 15. The frequency parameter β versus Winkler foundation stiffness $\bar{K}_w$ for moderately thick annular plate with both edges (outer and inner) free and thickness–radius ratio $\delta = 0.1$. (a) $(n, s) = (0, 1)$; (b) $(n, s) = (0, 2)$. (○) $R = 0.1$; (□) $R = 0.2$; (◇) $R = 0.3$; (▽) $R = 0.4$.

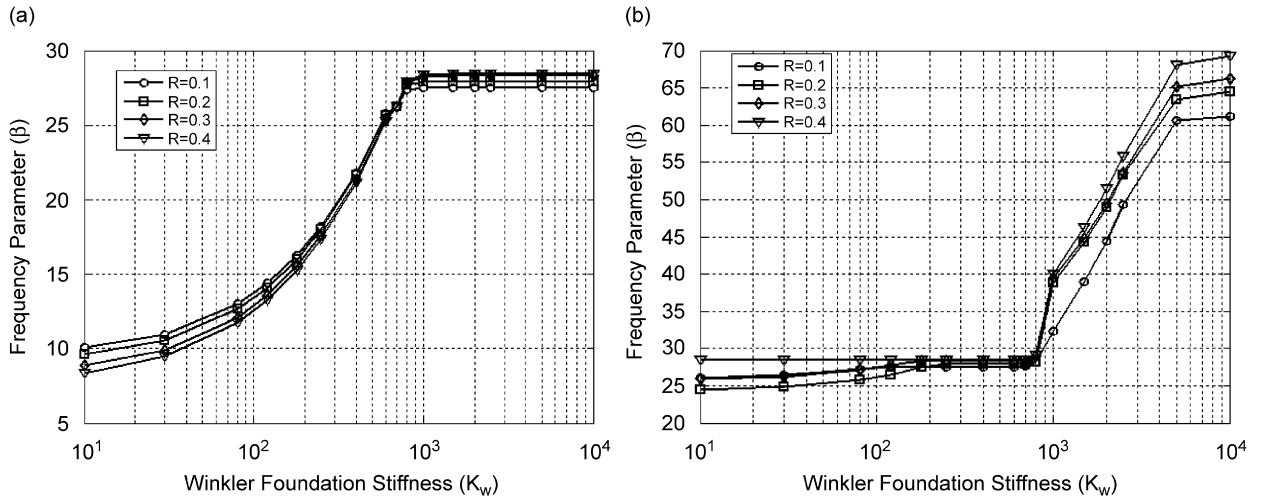

Fig. 16. The frequency parameter β versus Winkler foundation stiffness $\bar{K}_w$ for moderately thick annular plate with both edges (outer and inner) free and thickness–radius ratio $\delta = 0.1$: (a) $(n, s) = (1, 1)$; (b) $(n, s) = (1, 2)$. (○) $R = 0.1$; (□) $R = 0.2$; (◇) $R = 0.3$; (▽) $R = 0.4$.

In order to show the deflection of the thick annular plate resting on Pasternak foundation, 2-D plots and their corresponding 3-D mode shapes are depicted in Figs. 18–21 for the displacement components in the radial ($\bar{\psi}_1$), circumferential ($\bar{\psi}_2$) and thickness ($\bar{\psi}_3$) directions.

For each of four circumferential wavenumbers ($n = 0$, 1, 2, and 3), the first mode shape ($s = 1$) of a clamped–clamped annular plate ($R = 0.2$) resting on Pasternak foundation with thickness–radius ratio $\delta = 0.2$ and stiffness parameters $\bar{K}_w = 25$ and $\bar{K}_P = 2.5$ is illustrated in Fig. 18. In order to show thickness shear motion, the through-thickness mode shape of the displacement ($\bar{\psi}_3$) which is normalized by dividing its maximum value is plotted in Fig. 19 with respect to the non-dimensional coordinate $z^* = z/h$ when r^* is set to be 0.25. It is worth noting that the maximum thickness shear motion occurs in what value of z^* (see Table 9).

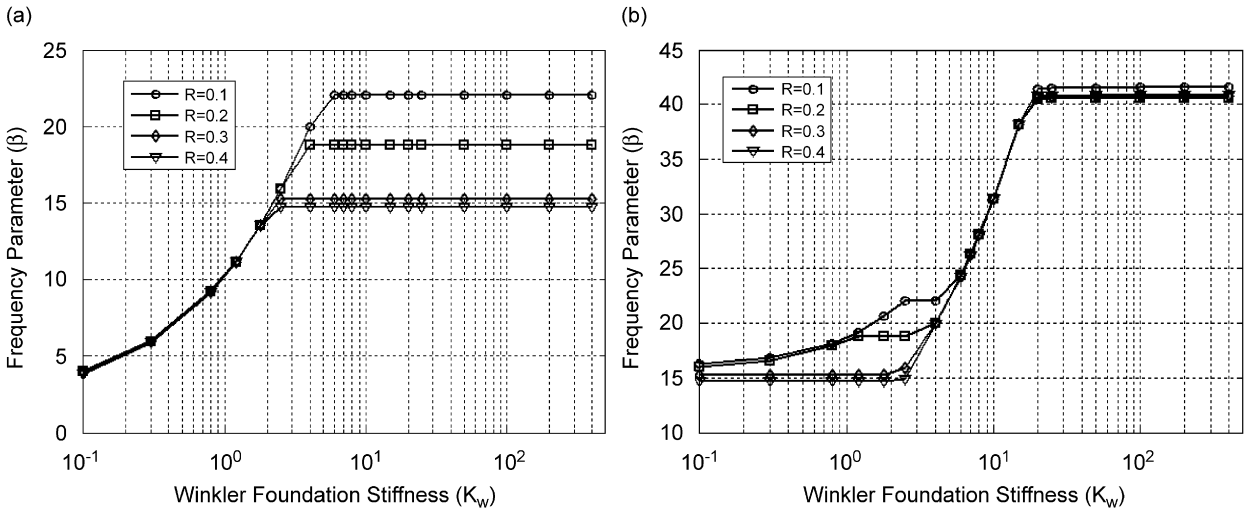

Fig. 17. The frequency parameter β versus Winkler foundation stiffness $\bar{K}_w$ for moderately thick annular plate with both edges (outer and inner) free and thickness–radius ratio $\delta = 0.1$: (a) $(n, s) = (2, 1)$; (b) $(n, s) = (2, 2)$. ($\circ$) $R = 0.1$; ($\square$) $R = 0.2$; ($\diamond$) $R = 0.3$; ($\triangledown$) $R = 0.4$.

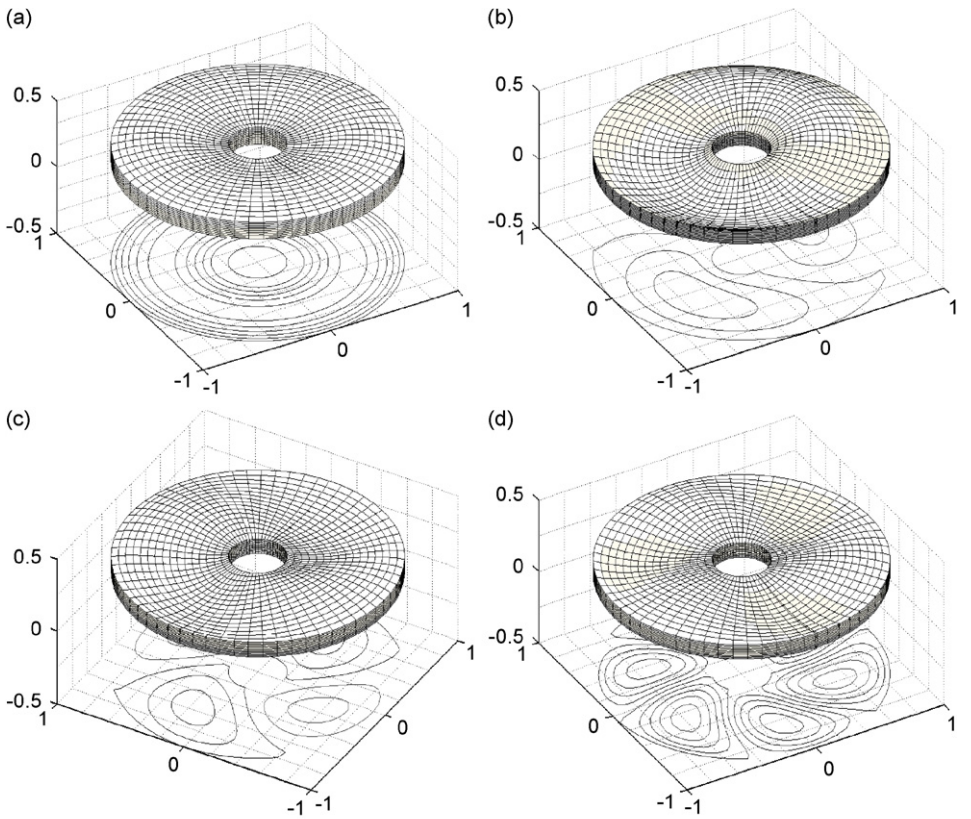

Fig. 18. Deformed mode shapes and frequency parameters of a clamped–clamped annular plate resting on Pasternak elastic foundation ($R = 0.2$, $\delta = 0.2$, $\bar{K}_w = 25$ and $\bar{K}_P = 2.5$). (a) Frequency parameter = 7.3898, mode (0, 1); (b) frequency parameter = 4.7088, mode (1,1); (c) frequency parameter = 5.7071, mode (2, 1); (d) frequency parameter = 6.8481, mode (3,1).

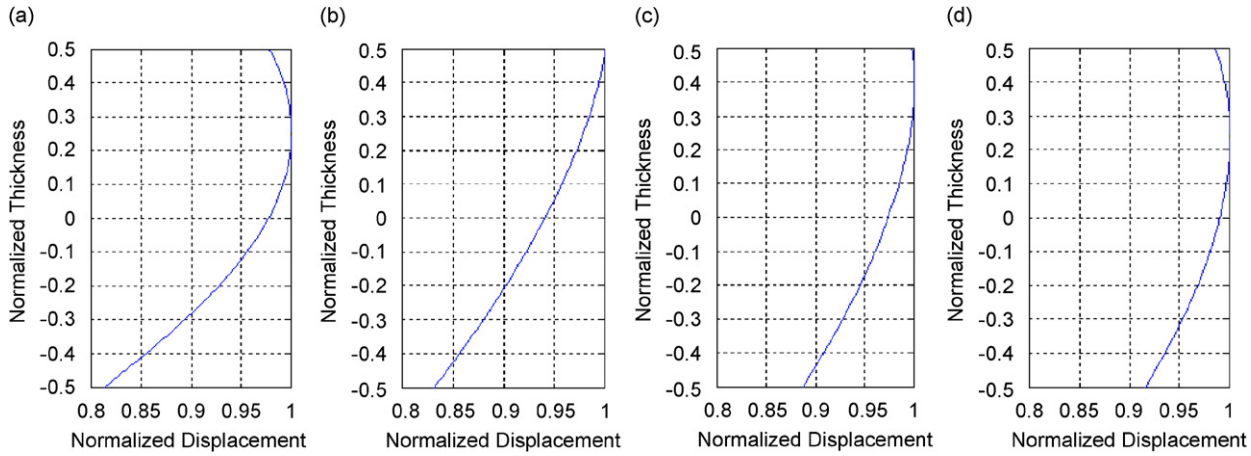

Fig. 19. Thickness mode shapes of the normalized displacement ($\bar{\psi}_3$) versus the normalized thickness (z^*) for the same annular plate mentioned in Fig. 18.

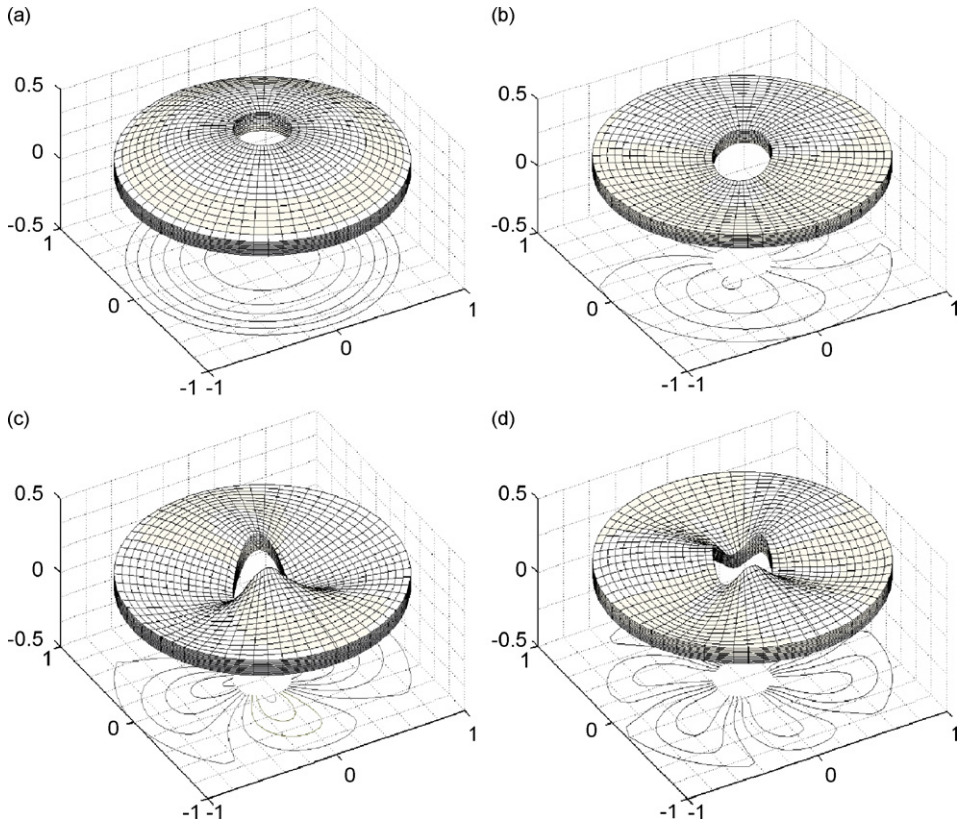

Fig. 20. Deformed mode shapes and frequency parameters of a clamped–free annular plate resting on Pasternak elastic foundation ($R = 0.2$, $\delta = 0.2$, $\bar{K}_w = 25$ and $\bar{K}_P = 2.5$). (a) Frequency parameter = 5.9929, mode (0, 1); (b) frequency parameter = 3.5690, mode (1,1); (c) frequency parameter = 4.3238, mode (2, 1); (d) frequency parameter = 6.2340, mode (3,1).

Figs. 20 and 21 presents deformed and thickness shape modes for the annular plate with the same values of ($\bar{K}_w, \bar{K}_P, \delta, R$) in Fig. 18 when the annular plate is constrained as a clamped–free in the outer and inner edges, respectively. Similarly, the amount of the maximum thickness shear motion for various vibrating modes (n, s) is presented in Table 9.

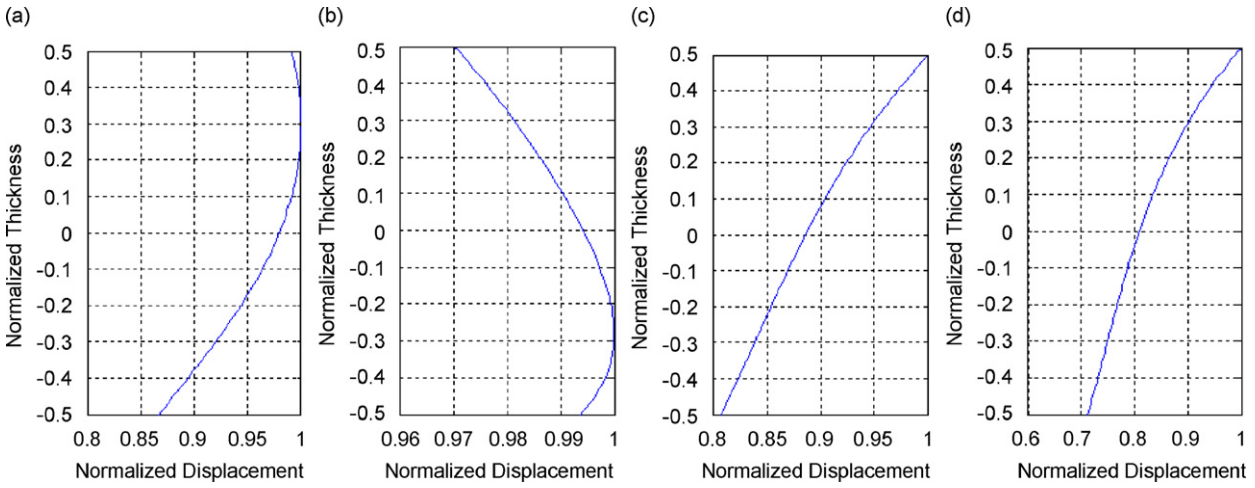

Fig. 21. Thickness mode shapes of the normalized displacement ($\bar{\psi}_3$) versus the normalized thickness (z^*) for the same annular plate mentioned in Fig. 18.

Table 9
The values of the normalized thickness z^* for occurring maximum shear thickness motion

Boundary conditions (outer–inner edges)	Normalized thickness z^*			
	(0, 1)	(1, 1)	(2, 1)	(3, 1)
Clamped–clamped	0.25	0.50	0.39	0.24
Clamped–free	0.32	−0.28	0.50	0.50

4. Conclusions

Based on the small strain and linear elasticity theory, a comprehensive study of the 3-D vibration analysis of annular plates resting on Pasternak elastic foundation with different combinations of free, soft simply supported, hard simply supported and clamped boundary conditions at the inner and outer edges was investigated. The Ritz method is applied to derive the eigenvalue equation. Due to the cylindrical nature of the annular plate geometry, the formulation was carried out in the cylindrical polar coordinates. Apart the convergence tests performed and the new results presented, the influence of different parameters of the annular plates on the ill-conditioning phenomenon in the mass matrix was studied and the exciting results were graphically presented. The success of the present analysis was also verified through comparisons with corresponding numerical results [23], the converged finite element solution results obtained using a well-known commercially available FEM package as well as the Mindlin results presented as a new study in this paper. The influence of the foundation stiffness parameters, thickness–radius ratio, inner–outer radius ratio and different combinations of boundary conditions on the frequency parameters of the annular plates was discussed. The validity and the range of applicability of the results obtained from the Mindlin and classical plate theories for thin and moderately thick annular plate with different values of the Winkler foundation stiffness parameter were determined through comparing them with those obtained from the present 3-D p-Ritz solution. It was proven that researchers would not be able to use the Mindlin and classical plate theories when the large values of the Winkler foundation stiffness are considered. Finally, 2- and 3-D plots of mode shapes were given for some vibrating modes. The 3-D mode shapes surround flexural, thickness twist and thickness shear motions. All of the results presented in this paper can be served as benchmark results for researchers to validate their numerical methods (i.e. classical and Mindlin theories as well as finite element method) and also for engineers to use such plates in their structures in the future.

Appendix A. The formulation of the Mindlin plate theory

A flat, isotropic and moderately thick annular plate with outer radius a_o, inner radius a_i, thicknesses h, Young's modulus E, shear modulus G, and Poisson ration v and resting on Pasternak elastic foundation is considered. The cylindrical coordinate system (r,θ,z) and geometry of plate is as defined in Fig. 1. In the Mindlin plate theory, three independent quantities namely W, Ψ_r and Ψ_θ are introduced to represent the deformations of the plate. For free vibration, W, Ψ_r and Ψ_θ have the following forms:

$$\begin{aligned}\Psi_r(r,\theta,t) &= -z\psi_1(r,\theta)\,e^{j\omega t},\\ \Psi_\theta(r,\theta,t) &= -z\psi_2(r,\theta)\,e^{j\omega t},\\ W(r,\theta,t) &= \psi_3(r,\theta)e^{j\omega t},\end{aligned} \tag{A.1}$$

where t is the time, ω denotes the natural frequency of vibration and $j=\sqrt{-1}$.

The Lagrangian energy functional $\mathbf{\Pi}$ of the Mindlin plate is defined as follows:

$$\mathbf{\Pi} = \mathbf{V}_{\max} - \mathbf{T}_{\max} + \bar{\mathbf{P}}. \tag{A.2}$$

Introducing the following non-dimensional coordinate

$$r^* = \frac{r}{a_o}, \quad \bar{\psi}_3(r,\theta) = W(r,\theta)/a_o, \tag{A.3}$$

$\mathbf{V}_{\max}, \mathbf{T}_{\max}$ and $\bar{\mathbf{P}}$ are given, respectively, by

$$\mathbf{V}_{\max} = \frac{D}{2a_o}\int_R^1\int_0^{2\pi}\left[\begin{array}{l}\left\{\left(\dfrac{\partial\bar{\psi}_1}{\partial r^*}\right)^2+\left(\dfrac{\bar{\psi}_1}{r^*}+\dfrac{\partial\bar{\psi}_2}{\partial\theta}\right)^2+\dfrac{2v}{r^*}\left(\dfrac{\partial\bar{\psi}_1}{\partial r^*}\right)\left(\dfrac{\bar{\psi}_1}{r^*}+\dfrac{\partial\bar{\psi}_2}{\partial\theta}\right)\right\}\\ \quad+\dfrac{(1-v)}{2r^{*2}}\left(\dfrac{\partial\bar{\psi}_1}{\partial\theta}+r^*\dfrac{\partial\bar{\psi}_2}{\partial r^*}-\bar{\psi}_2\right)^2\\ \quad+\dfrac{6(1-v)K^2}{\delta^2}\left\{\left(\dfrac{\partial\bar{\psi}_3}{\partial r^*}-\bar{\psi}_1\right)^2+\left(\dfrac{\partial\bar{\psi}_3}{r^*\partial\theta}-\bar{\psi}_2\right)^2\right\}\end{array}\right] r^*\,d\theta\,dr^*, \tag{A.4}$$

$$\mathbf{T}_{\max} = \frac{1}{2}\rho\omega^2 a_o^3 h\int_R^1\int_{-1/2}^{1/2}\left\{\frac{\delta^2}{12}(\bar{\psi}_1^2+\bar{\psi}_2^2)+\bar{\psi}_3^2\right\}r^*\,d\theta\,dr, \tag{A.5}$$

$$\bar{\mathbf{P}} = \frac{1}{2}\rho\omega^2 a_o^3 h\int_R^1\int_{-1/2}^{1/2}\left\{\frac{\delta^2}{12}(\bar{\psi}_1^2+\bar{\psi}_2^2)+\bar{\psi}_3^2\right\}r^*\,d\theta\,dr, \tag{A.6}$$

in which, ρ is the plate density per unite volumes, $D=Eh^3/[12(1-v^2)]$ is flexural rigidity of plate, K^2 is the shear correction factor, $\delta=h/a_o$ is the thickness–radius ratio of the plate, $\bar{K}_w=k_w a_0^4/D$ is the Winkler foundation stiffness and $\bar{K}_P=k_p a_0^2/D$ is constant showing the effect of shear interaction of the vertical elements.

The transverse and rotations may be approximate by set of two dimensional polynomial that is function in (r,θ) plan as

$$\begin{aligned}\bar{\psi}_1(r^*,\theta) &= \cos(n\theta)G_1(r^*)\sum_{i=0}^{N_1}a_i(r^*)^i,\\ \bar{\psi}_2(r^*,\theta) &= \sin(n\theta)G_2(r^*)\sum_{i=0}^{N_1}b_i(r^*)^i,\\ \bar{\psi}_3(r^*,\theta) &= \cos(n\theta)G_3(r^*)\sum_{i=0}^{N_1}c_i(r^*)^i,\end{aligned} \tag{A.7}$$

Table A1
Boundary functions for different boundary conditions

Boundary condition	$G_1(r^*)$	$G_2(r^*)$	$G_3(r^*)$
Free edge (F)	1	1	1
Simply supported (S)	1	1	(r^*-1)
Clamped boundary condition (C)	(r^*-1)	(r^*-1)	(r^*-1)

where the non-negative integer n represents the circumferential wavenumber of the corresponding mode shape; a, b and c are the corresponding unknown coefficients associated with Ritz function. and $G_1[r^*]$, $G_2[r^*]$, and $G_3[r^*]$ are basic function corresponding to $\bar{\psi}_1$, $\bar{\psi}_2$ and $\bar{\psi}_3$ respectively. The basic functions are chosen to satisfy geometric boundary conditions, as shown in Table A1.

The eigenvalue problem is formulated by minimizing the free vibration frequencies with respect to the arbitrary coefficients a_i, b_i and c_i. Minimizing the above functional with respect to the coefficients, i.e.

$$\frac{\partial \mathbf{\Pi}}{\partial a_{ij}} = 0, \quad \frac{\partial \mathbf{\Pi}}{\partial b_{ij}} = 0, \quad \frac{\partial \mathbf{\Pi}}{\partial c_{ij}} = 0, \tag{A.8}$$

lead to the following eigenfrequency equation,

$$(\mathbf{K} - \beta^2 \mathbf{M})\mathbf{C} = \mathbf{0}, \tag{A.9}$$

where

$$K = \begin{bmatrix} \mathbf{k_{11}} & \mathbf{k_{12}} & \mathbf{k_{13}} \\ & \mathbf{k_{22}} & \mathbf{k_{23}} \\ \text{sym} & & \mathbf{k_{33}} \end{bmatrix}, \quad \mathbf{M} = \begin{bmatrix} \mathbf{m_{11}} & 0 & 0 \\ & \mathbf{m_{22}} & 0 \\ \text{sym} & & \mathbf{m_{33}} \end{bmatrix}, \quad \mathbf{C} = \begin{Bmatrix} \mathbf{a} \\ \mathbf{b} \\ \mathbf{c} \end{Bmatrix}. \tag{A.10}$$

References

[1] W. Lessia, NASA SP 160, Vibration of Plates, 1969.
[2] T. Irie, G. Yamada, S. Aomura, Natural frequencies of Mindline circular plates, *Journal of Applied Mechanics* 47 (1980) 652–655.
[3] J. So, A.W. Leissa, Three-dimensional vibrations of thick circular and annular plates, *Journal of Sound and Vibration* 209 (1998) 15–41.
[4] K.M. Liew, B. Yang, Elasticity solutions for free vibrations of annular plates from three-dimensional analysis, *International Journal of Solids and Structures* 37 (2000) 7689–7702.
[5] H. Rokni Damavandi Taher, M. Omidi, A.A. Zadpoor, A.A. Nikooyan, Free vibration of circular and annular plates with variable thickness and different combinations of boundary conditions, *Journal of Sound and Vibration* 296 (2006) 1084–1092.
[6] K.M. Liew, B. Yang, Elasticity solutions for free vibrations of annular plates from three-dimensional analysis, *International Journal of Solids and Structures* 37 (2000) 7689–7702.
[7] D. Zhou, F.T.K. Au, Y.K. Cheung, S.H. Lo, Three-dimensional vibration analysis of circular and annular plates via the Chebyshev–Ritz method, *International Journal of Solids and Structures* 40 (2003) 3089–3105.
[8] M.M. Filonenko-Borodich, Some approximate theories of the elastic foundation, *Uchenyie Zapiski Moskovskogo Gosudarstuennogo Universiteta Mechanika* 46 (1940) 3–18 (in Russian).
[9] P.L. Pasternak, On a new method of analysis of an elastic foundation by means of two foundation constants, Gosudarstvennoe Izdatelstvo Literaturi po Stroitelstvu i Arkhitekture, Moscow, 1954 (in Russian).
[10] A.D. Kerr, Elastic and viscoelastic foundation models, *Journal of Applied Mechanics* 31 (3) (1964) 491–498.
[11] V.Z. Vlasov, U.N. Leontev, *Beams, Plates and Shells on Elastic Foundations* (translated from Russian), Israel Program for Scientific Translation Jerusalem, Israel, 1966.
[12] R. Bolton, Stresses in circular plates on elastic foundations, Proceedings of the American Society of Civil Engineers, *Journal of the Engineering Mechanics Division* 98 (1972) 629–640.
[13] E. Winkler, Die Lehre von der Elasticitaet und Festigkeit, Prag. Dominicus, 1867.
[14] P.C. Dumir, Non-linear vibration and post buckling of isotropic thin circular plates on elastic foundation, *Journal of Sound and Vibration* 107 (2) (1986) 253–263.
[15] A.W. Leissa, *Vibration of Plates*, Acoustical Society of America, Sewickley, PA, 1993.

[16] M. Salari, C.W. Bert, A.G. Striz, Free vibration of a solid circular plate free at its edge and attached to a Winkler foundation, *Journal of Sound and Vibration* 118 (1987) 188–191.
[17] U.S. Gupta, R. Lal, R. Sagar, Effect of an elastic foundation on axisymmetric vibrations of polar orthotropic Mindlin circular plates, *Indian Journal of Pure and Applied Mathematics* 25 (1994) 1317–1326.
[18] F. Ju, H.P. Lee, K.H. Lee, Free vibration of plates with stepped variations in thickness on non-homogeneous elastic foundations, *Journal of Sound and Vibration* 183 (1995) 533–545.
[19] U.S. Gupta, R. Lal, S.K. Jain, Effect of elastic foundation on axisymmetric vibrations of polar orthotropic circular plates of variable thickness, *Journal of Sound and Vibration* 139 (1990) 503–513.
[20] U.S. Gupta, A.H. Ansari, Effect of elastic foundation on axisymmetric vibrations of polar orthotropic linearly tapered circular plates, *Journal of Sound and Vibration* 254 (3) (2002) 411–426.
[21] P.A.A. Laura, R.H. Gutierrez, Free vibrations of a solid circular plate of linearly varying thickness and attached to Winkler foundation, *Journal of Sound and Vibration* 144 (1991) 149–161.
[22] K.M. Liew, J.B. Han, Z.M. Xiao, H. Du, Differential quadrature method for Mindlin plates on Winkler foundations, *International Journal of Mechanical Sciences* 38 (4) (1996) 405–421.
[23] D. Zhou, S.H. Lo, F.T.K. Au, Y.K. Cheung, Three-dimensional free vibration of thick circular plates on Pasternak foundation, *Journal of Sound and Vibration* 292 (2006) 726–741.
[24] A.Y.T. Leung, B. Zhu, J. Zheng, H. Yang, Analytic trapezoidal Fourier p-element for vibrating plane problems, *Journal of Sound and Vibration* 271 (2004) 67–81.